EXPERIMENTAL TESTS OF AN ELECTRO-ANATOMICAL MODEL OF THE RAT'S COCHLEA

by

Christopher Warren McKinney

SUBMITTED IN PARTIAL FULFILLMENT OF
THE REQUIREMENTS OF THE DEGREES OF

BACHELOR OF SCIENCE and
MASTER OF ENGINEERING
in ELECTRICAL ENGINEERING AND
COMPUTER SCIENCE

at the

MASSACHUSETTS INSTITUTE OF
TECHNOLOGY
May 1995

Signature of Author _____

Department of Electrical Engineering and Computer Science
May 26,1995

Certified by _____

Robert D. Hall, Ph.D.
Thesis Supervisor

Accepted by _____

F. R. Morgenthaler
Chairman, Departmental Committee on Graduate Students

Experimental Tests of an Electro-Anatomical Model of the Rat's Cochlea

by

Christopher W. McKinney

Submitted to the

Department of Electrical Engineering and Computer Science

May 26, 1995

In partial fulfillment of the Requirements for the Degrees of

Bachelor of Science and Master of Engineering in

Electrical Engineering and Computer Science

Abstract

An electro-anatomical model of the rat's cochlea was tested to determine the accuracy of the potential distributions the model predicts with current stimulation. Monopolar and bipolar potential measurements were made at five intracochlear electrodes in both chronically and acutely implanted rats. Some measurements were made to test some of the underlying assumptions of the model: conformance of the implanted cochlea to basic circuit laws, system linearity, and independence of stimulus frequency. In other experiments monopolar potential distributions were compared with model predictions. Other issues, such as the effect of time and tissue growth in chronically implanted subjects and the effects of death on potential measurements, were also investigated. The basic assumptions of the model were validated and the death experiments provided preliminary evidence that an *in vitro* preparation may be feasible. For the most part, the model predictions were found to be in good agreement with the experimental data, but some interesting exceptions will require some novel implementations of the model that have not yet been run.

Thesis Supervisor: Dr. Robert D. Hall

Title: Director, Auditory Prosthesis Research Laboratory, MEEI

Acknowledgements

I would like to thank Dr. Robert D. Hall for his excellent guidance and total involvement in this research. He spent many late hours in the laboratory troubleshooting equipment, many afternoons commenting on drafts of this document, and countless other days simply providing sound advice about the direction my research should take. His influence has given me a new idea about ways to do good research, and his thorough analysis of my writing has shown me the importance of clarity and organization in technical writing. I certainly hope that he has seen the same improvements that I have. Thanks, Bob.

Dr. Donald Eddington provided many helpful insights during all phases of this research. His input often helped me understand the meaning of some of my data and how they should direct my collection of data in the future. Without Drs. Eddington and Hall, this research would not have been possible and I could not have experienced the most rewarding technical experience of my life.

Dr. Meng-Yu Zhu spent many days working with the model software and producing the model predictions presented here. Her assistance analyzing the model data and comparing it to experimental data is greatly appreciated.

Dr. Wen Z. Xu was extremely helpful while doing all histological work presented in this thesis. He also helped brighten many discouraging days in the laboratory with encouraging comments and frequent questions about the progress of my work.

I would like to thank my parents, Douglas and Pauline McKinney, for emotional and financial assistance over the last five years. More importantly, I want to thank them for a lifetime of influences that have produced the person I am today. My graduation from MIT is one of my most significant personal achievements and I know it will make them proud. Mom and dad, I love you both.

I would like extend graditude to Scott Paxton, Thomas Pinckney, Andrew Stark, and Dorian Balch. I have known each of them for a substantial portion of my time here and each has added to my experience here in his own unique manner. As a whole, they have driven me when I started to slack, they have forced me to be calm when I became stressed, and they have provided the friendships that made MIT more than just a great place to get a technical education. I hope that my influence upon them has provided many of the same benefits, for this is the only method of repayment I can imagine.

Finally, I would like to thank Laura R. Bates for the sanity that she helped maintain during the final months of this project. She never allowed me to get discouraged and was constantly pointing out that "my thesis is going great!" She never complained while listening to my endless stories, both positive and negative, about my life and even showed interest in the minute details that even I did not recognize. I hope that she does not underestimate her importance, and that she realizes how much more difficult the last six months would have been without her presence. Thank you, Laura.

Contents

List of Figures

List of Tables

1 Introduction

Cochlear prostheses are devices that transform acoustic stimuli into electrical signals that are used to stimulate directly the auditory nerve of people who are profoundly deaf. The electrical stimuli provide auditory information to those who would otherwise be unable to hear. The devices currently in use are mainly multichannel systems that employ a variety of electrode arrays containing from four to twenty-two electrodes. Various schemes are used for encoding acoustic signals, most importantly speech, into electrical signals for presentation across the electrode arrays.

The benefits obtained from present implants are quite variable. Nearly every patient can interpret most environmental sounds. Some patients hear well enough to converse on the telephone, while others experience only a slight increase in lip-reading ability. The Massachusetts Eye and Ear Infirmary (MEEI) and the Research Laboratory of Electronics (RLE) at MIT are trying to improve cochlear prostheses by furthering the understanding of how electrical stimuli excite auditory afferent neurons. One step in this effort is modeling the electrical properties of the cochlea to achieve useful descriptions of the patterns of current flow that result from various patterns of stimulation. This is a first step in attempting to predict the spatio-temporal patterns of activation across populations of auditory nerve fibers with intracochlear stimulation. The ability to do this could guide the design of new electrode arrays and processors that encode speech.

An electrical model of the human cochlea is very difficult to develop because the cochlea is a small, complex structure. The spiraling basilar membrane is about 34 mm long in humans, and the axis of the spiral is about 4 mm long. Mammalian cochleas are quite similar across species, differing mainly in size. Figure 1 shows a drawing of a cross-section of a rat's cochlea. The cochlea's most prominent structures are three fluid filled tubes, called scala vestibuli, scala tympani, and scala media. The scalae run parallel to each other along the entire length of the cochlea, spiraling around the bony modiolus. Scala vestibuli is separated from scala media by the very thin Reisner's membrane. Scala tympani is separated from scala media by the basilar membrane, which supports the organ of Corti. Scala tympani and scala vestibuli are joined at the most apical point of the cochlea, the helicotrema. The outer end of the basilar membrane and Reisner's membrane are attached to the spiral ligament

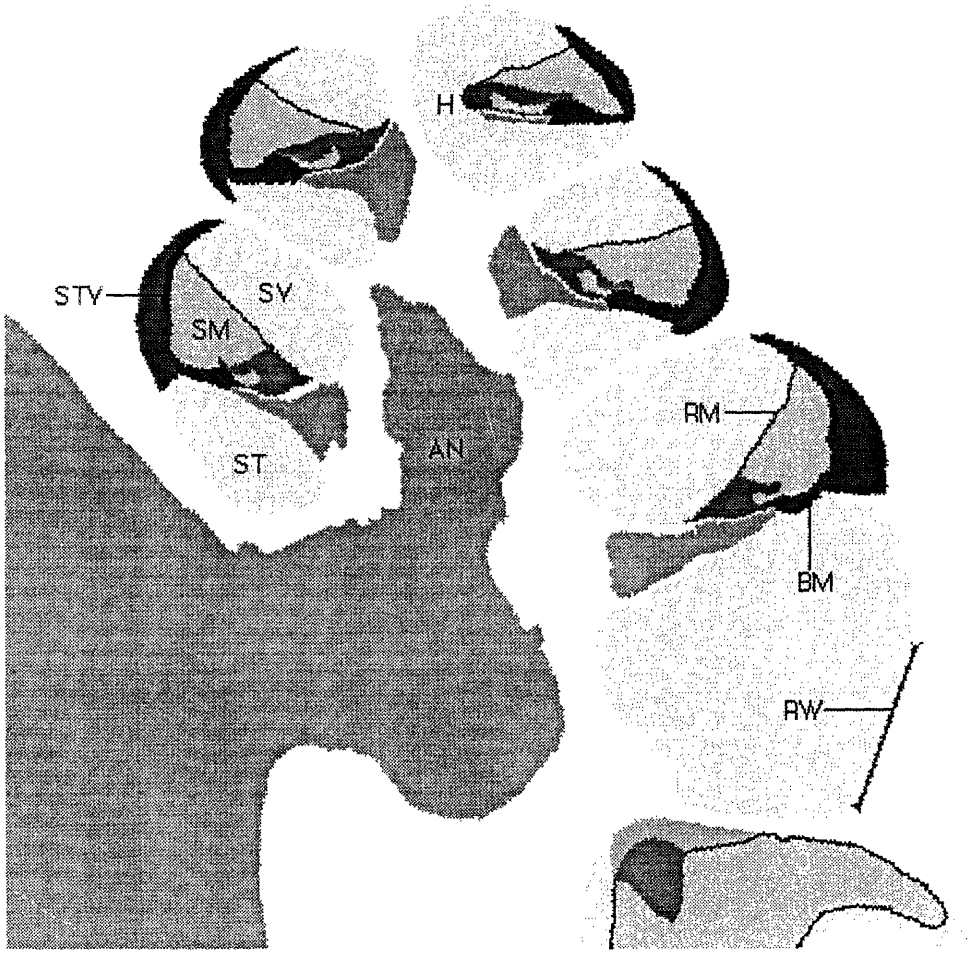

Figure 1: Cross section of the rat cochlea as seen in the drawings that comprise the morphological basis of the electro-anatomical model. Several structures are denoted as follows: SM = scala media, ST = scala tympani, SV = scala vestibuli, STV = stria vacularis, RM = Reisner's membrane, BM = basilar membrane, RW = round window membrane, and AN = auditory nerve. Courtesy of Dr. Robert D. Hall.

and the cells of the stria vascularis, a specialized part of the spiral ligament, are responsible for the maintenance of the high concentration of potassium ions (K^+) in the endolymph, the fluid that fills scala media. Figure 2, which is a three-dimensional rendering based on two-dimensional drawings of the rat cochlea, provides some appreciation for the three-dimensional structure of the cochlea, especially the spatial arrangement of the scalae.

In a normal ear, sound is transmitted to the cochlea through the ossicles of the middle ear, ending with pressure applied by the stapes on the fluid of scala vestibuli. The pressure is transmitted by scala vestibuli toward the helicotrema, and back to the basal extreme of scala tympani. This traveling

pressure wave causes movement of the basilar membrane, which in turn results in stimulation of the cochlear hair cells located along its length. Activation of the hair cells leads to excitation of the auditory nerve fibers which convey the information about the acoustic stimulus to the brain. In sensorineural deafness, it is most often the loss of hair cells that interupts the chain of events leading to the perception of sound. Cochlear implants attempt to correct that deficit by stimulating the auditory nerve directly after encoding the acoustic stimuli as electrical stimuli. The problem in doing this with much fidelity is that it is not possible to stimulate the roughly 30,000 fibers of the auditory nerve individually. The stimuli are of necessity applied through large electrodes in a highly conductive medium, the perilymph of scala tympani. It is difficult to know what fibers are being stimulated under particular stimulus conditions because our knowledge of the patterns of current flow is still rather primitive.

Previous electrical models of the cochlea have been generally similar to von Bèkèsy's early lumped-parameter transmission line model (von Bèkèsy, 1951). Girzon's (1987) review points out that a number of the electrical properties of the cochlea were revealed through these efforts, including the well insulated scala media, the relatively small resistance between scala tympani and scala vestibuli through the spiral ligament, the electrical isolation of the cochlea resulting from the bony capsule surrounding it, and the grounding of the cochlea mainly through the auditory nerve and blood vessels exiting it in the internal auditory meatus. However, the resolution of these lumped-parameter models was not adequate to determine local patterns of current flow in the vicinity of the nerve fiber, which is of prime importance for cochlear implant considerations. The transmission line models also "unwind" the cochlea and do not deal with it in three dimensions, thereby ignoring the possibility of cross-turn coupling and oversimplifying the ground pathways. Advances in the cochlear implant field and the subsequent increase in implant use have resulted in the need for a high resolution model of the cochlea. The model currently being developed at the MEEI is a finite element model of the human cochlea and is the model put forth in Gary Girzon's MS thesis at MIT (Girzon, 1987). The model was originally conceived by Donald K. Eddington of the Cochlear Implant Research Laboratory at MEEI and the Research Laboratory of Electronics.

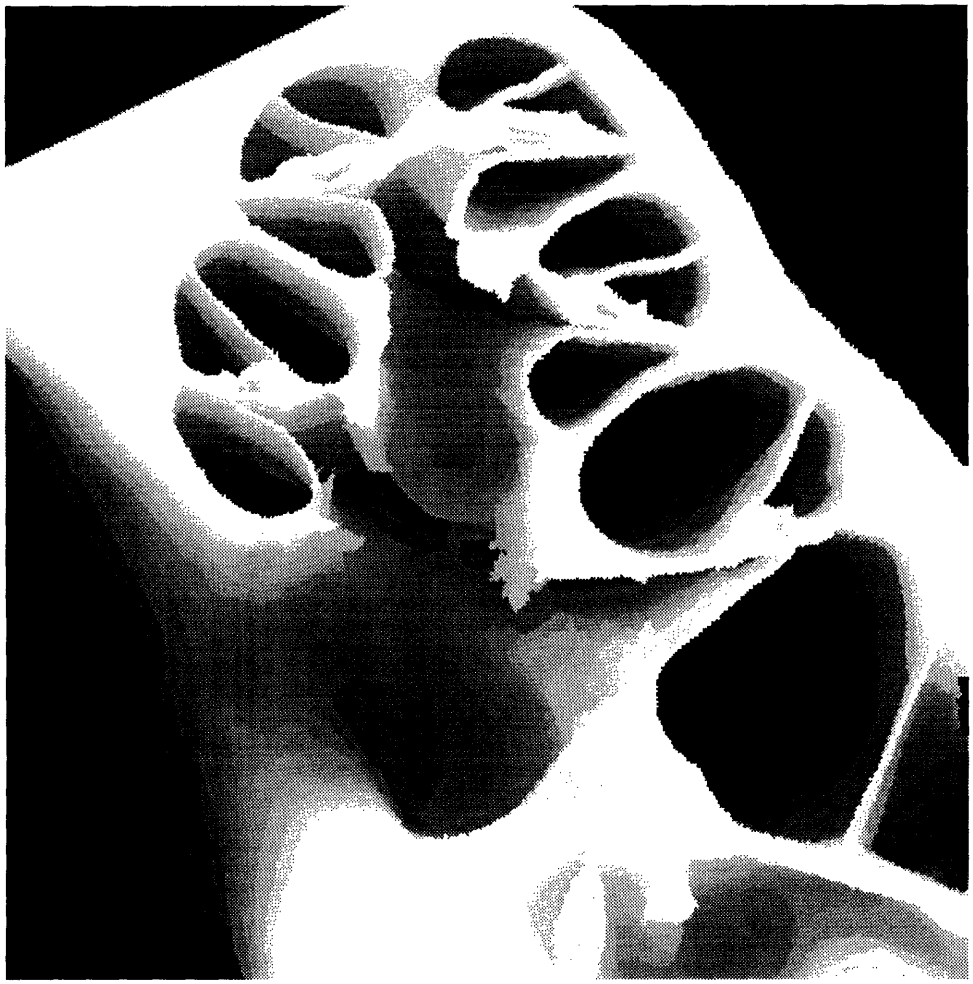

Figure 2: 3-D rendering of the rat cochlea constructed from a partial series of histological sections beginning in an approximately mid-modiolar plane. Courtesy of Dr. Meng-Yu Zhu.

In the model, the cochlea is composed of many small "bricks", each one representing a particular type of tissue or fluid. The organization of the bricks was derived from histological sections of the cochlea. Outlines of the structures in each cross section of the cochlea have been drawn using various techniques, most recently using digital images of sections captured by a video-microscope camera. Each brick within the boundaries of a given structure was assigned a tag representing the specific resistance of that kind of tissue or fluid as reported in the literature. The resulting meshes, each of which was only one brick thick, were stacked to form a three-dimensional mesh. The model is implemented by solving simultaneous equations for the potential and current at the center of each brick face. The resolution can be varied, so the size of the bricks and the time required to solve the equations is controlled by the model user. This model of the cochlea is the first one to be based upon a relatively high resolution morphology.

The Eddington-Girzon model has been tested in patients with cochlear implants. Both monopolar stimulation (stimulation between one intracochlear electrode and a reference electrode elsewhere on the body) and bipolar stimulation (stimulation between two intracochlear electrodes) were used, and the potentials at the other intracochlear electrodes were measured. These potential measurements were compared to data generated by the model. The two sets of data were generally in good agreement (Girzon, 1987).

The amount of testing that is possible in humans is limited by several factors, the electrode array being the most important. Because all electrodes are inserted through the round window, all electrodes reside in scala tympani, their positions along scala tympani being fixed by the design of the devices approved by the Food and Drug Administration. Ethical limitations also limit human experimentation to completely non-injurious techniques. Consequently, manipulations of the cochlea for experimental analysis are not possible (for example, introducing some impediment to current flow in a particular direction).

To obtain the advantages of an animal model, the Eddington-Girzon electro-anatomical model of the cochlea is being extended to the rat, as the principal difference between the cochleas of most laboratory animals and the human cochlea is size. The animal cochleas are significantly smaller

than that of the human. For example, the basilar membrane in the rat is only about 11 mm long, approximately one-third the length of the human basilar membrane, and the length of the cochlea along its axis is only about 2 mm.

The rat was chosen because it is being used in the Auditory Prosthesis Research Laboratory (APRL) to address a number of fundamental issues in cochlear implant research and because many techniques required for the testing were already in hand. The structural basis for the rat model was completed in the APRL. Dr. Meng-Yu Zhu of the CIRL has modified the computer software used for solving Girzon's human model so that the rat model may be implemented. The rat model is based on horizontal 5-μm sections of the cochlea and ajoining structures. Every tenth section was drawn, making the resolution of the model 50 μm in the ventrodorsal plane (z-axis). Each section was captured as a digital image, 640 x 480 pixels with a resolution of 6.25 μm. The method of tagging the model bricks with resistivities was similar to that used in the human model. A representative section used in developing the rat model was shown in Figure 1. When the thin meshes were overlayed to form the 3-D model, some structures did not join properly from section to section. The most notable case of this problem was Reisner's membrane separating scala vestibuli from scala media. This membrane is so thin (a few μm) that small changes in its position in non-serial histological sections resulted in gaps from section to section that were larger than one brick. The membrane was redrawn by hand in these sections to close the holes in Reisner's membrane that would have otherwise electrically connected scala vestibuli and scala media. The model domain extends beyond the walls of the cochlea and into the surrounding tissues and spaces: the air filled space of the middle ear, the cerebellum and brain stem, and the ampullae and vestibule of the vestibular system. Resistivities for the structures encompassed by the model were assigned using reported values from published research, or they were estimated when no published measurements were available. A total of 22 different structures and their potentially different resistivities were distinguished in the drawings, but for the initial implementations of the model presented here, the resistivities have been reduced to six different values by assigning identical resistivities to tissues with presumably similar resistivities. The brain stem occupies a large space at the edge of the model

domain. Because there is considerable evidence that with monopolar stimulation current leaves the cochlea mainly through the auditory nerve and blood vessels in the internal auditory meatus to the brainstem and surrounding fluid, the brainstem was chosen as the zero potential point in the present model implementation.

The purpose of this research is to test the Eddington-Girzon model, as it has been extended to the rat cochlea. To do so, the potential distributions were measured when currents were injected through electrodes implanted at five intracochlear locations. Various stimuli, both monopolar and bipolar, were presented at several frequencies to explore the question of whether capacitive properties of the tissues influence the potential distributions. In some experiments, it was also possible to address the question of whether the differences between the ground location in the experimental situation, the ipsilateral pinna, and the computer simulation, the brainstem, might influence the results.

2 Methods

2.1 Subjects

Intracochlear electrodes were surgically implanted in twenty-one male rats from the Long-Evans strain ranging in age from 2 to 6 months, weighing 254 g to 683 g. The Long-Evans strain was chosen because it is a pigmented wild-type strain that is being used in the APRL for cochlear implant research.

The animals were anesthetized initially with 2 mL of a mixture of ketamine HCl, rhompun, and acepromazine per 1 kg body weight. Ketamine was used as the initial anesthetic because it is a strong anesthetic without the depressive side effects of barbiturate anesthetics. Doses of sodium pentobarbital (approximately 40 mg/kg every hour) were used as necessary to maintain a surgical level of anesthesia throughout the procedure.

The dorsal surface and the left lateral surface of the skull were exposed down to the external ear canal. The ear canal was detached from the bulla to expose the external auditory meatus and the tympanic membrane. A dental burr was used to enlarge the external meatus, removing much of the ventral and posterior portions of the bulla, the bony cavity that encompasses the middle ear. The tympanic membrane, malleus, incus, and tensor tympani were removed to expose the lateral face of the cochlear capsule. The stapes was left intact to avoid damaging the oval window membrane or the stapedial artery, which runs through a hole in the stapes.

The posterior portions of the bulla were removed, with care taken to avoid damaging the facial nerve, which courses over the bone that borders the round window laterally. The thicker section of that bone was removed to expose the round window. With the cochlea completely exposed, the dorsal aspect of the bulla was removed to allow easier access from above during electrode placement.

2.2 Rationale for Electrode Placement

Electrode placement was determined by several factors, including ease of approaching the cochlea, accessibility of scala tympani, and a desire to distribute the electrodes rather evenly along the length

of the scala. Scala tympani was chosen as the site for most electrodes in these measurements to make them comparable to the measurements made in humans whose electrodes are in scala tympani in most current devices. An array of five electrodes was chosen to maximize the number of points available for stimulation and recording without causing excessive damage to the cochlea.

Scala tympani was found to be easily approached only from above, along the dorsal crest of the cochlea. Along the crest, scala tympani lies posterior to scala media, just beneath the capsule. Elsewhere, it is more or less obscured by scala media, scala vestibuli, or the interscalar septum.

Figure 3 is a schematic representation of the midpoint of scala tympani based upon the drawings of the histological sections. Dr. Meng-Yu Zhu made this representation by determining the midpoint of scala tympani in each of the model sections, recording its coordinates, and then plotting these positions on two dimensional graphs. Estimations of the distances between points in sucessive sections were made using the formula $\Delta \mathrm{d} = \sqrt{\Delta x^2 + \Delta y^2 + \Delta z^2}$, where Δx, Δy, and Δz are the changes in x, y, and z coordinates, respectively, from one section to the next. These distances were summed to estimate the distances from the round window to the most dorsal midpoints of the two turns of scala tympani, approximately 3.9 mm and 7.1 mm, respectively, and the helicotrema, 8.0 mm, the intended sites of three electrodes. The helicotrema was chosen as an appropriate point for electrode implantation because, in addition to being accessible from the lateral direction, it is the junction of scala vestibuli and scala tympani. Though this point is effectively in both scalae, it also represents the most apical point of scala tympani. The 8.0 mm distance is significantly smaller than the previously published length of the cochlea, approximately 11 mm (Burda et al., 1988) because the 11 mm was measured along the basilar membrane. When the length of the basilar membrane was measured using Dr. Zhu's representation, it was 11.7 mm.

Two electrodes were inserted into scala tympani through the round window. The insertion distance of the deeper electrode was limited by the stiffness of the electrode wire and the short radius of the cochlea. The most ventral midpoint of scala tympani, where the scala turns, was found to be about 1.5 mm from the round window. This point was chosen as the goal for electrode placement because it was feared that further insertion would lead to cochlear damage because the electrode

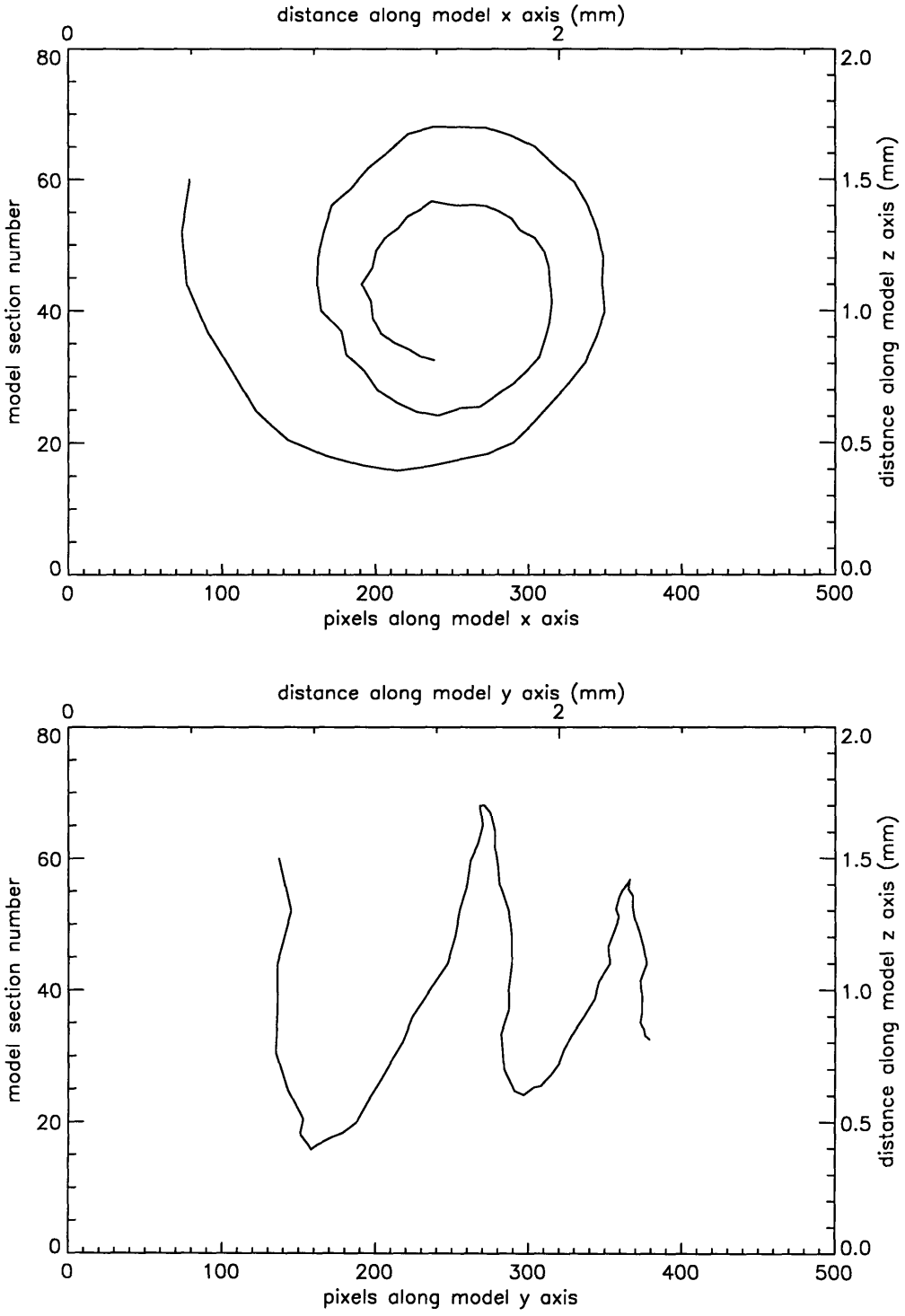

Figure 3: Schematic representation of the midpoint of scala tympani. Courtesy of Dr. Meng-Yu Zhu

wire would not bend and remain in scala tympani. Another electrode was placed immediately inside the round window at the most basal point of the cochlea. Table 1 summarizes the electrode names that were assigned, along with the distance from the round window (RW) along scala tympani (ST).

Table 1: Intended Electrode Positions in Scala Tympani

Electrode Position in ST	Distance from RW along ST
Apical	8.0 mm
Mid-Apical	7.1 mm
Mid-Basal	3.9 mm
Basal	1.5 mm
RW	0.0 mm

2.3 Electrode Implantation

The wire used for the electrodes is made from a platinum-iridium (Pt-Ir) alloy that is insulated with teflon. The diameter of the wire is 0.03 inches ($\cong$ 75 μm) when bare and 0.045 inches ($\cong$ 115 μm) when insulated. The electrode tips were prepared by removing the wire insulation from the tip with a flame and then cutting them to leave approximately 100 μm of bare wire. This cylindrical tip was used for all electrodes except the basal electrode. A ball tip was constructed for this electrode by heating the tip of the bare wire with flame until it melted. The heat was removed and the electrode quickly solidified with a spherical tip. This tip was deemed more appropriate for insertion deep into scala tympani because it would be less damaging to the soft tissues lining the scala.

The apical, mid-apical, and mid-basal electrodes were inserted through holes drilled in the capsule with an insect pin mounted in a pin vise modified to fit a Foredom drill. Attempts were made to drill the mid-apical and mid-basal holes near the posterior edge of the stria vascularis, which is frequently seen through the thin bone of the capsule, as it passes the dorsal crest of the cochlea. The stria vascularis lies over scala media, so attempts were made to avoid drilling the stria while drilling as close to it as possible. The apical electrode hole was drilled at the most apical tip of the cochlea. The cochlear capsule is approximately 50 μm thick, so extreme care was taken to drill holes that were barely large enough for electrode insertion to avoid cracking the capsule.

The basal and round window electrodes were implanted first and cemented in place with carboxylate dental cement. The other electrodes were implanted and cemented separately. The electrode wires were cemented to the lateral wall of the skull and connected to five pins of a 9-pin electrical connector (ITT Cannon MD1-9PL1), which was held to the dorsal surface of the skull by stainless steel screws and a dental acrylic cement. The rat's wounds were sutured at the completion of the surgical procedure.

2.4 Stimulus Generation and Isolation

The stimuli presented to the rat cochlea were generated with the Signal Averaging software and hardware manufactured by Modular Instruments, Inc. under control by a computer running MS-DOS. The stimuli were sinusoidal bursts of current with 2-cycle rise and fall times and 5-cycle plateaus. Three different frequencies were used - 100 Hz, 1 kHz, and 10 kHz - to determine if there were any capacitive or inductive effects inside the cochlea. The bursts were presented at a rate of 5/s when f = 100 Hz, or 50/s when f = 1 kHz or 10 kHz. The peak amplitude of each stimulus was 10 μA except when amplitude was the experimental variable.

The stimuli were isolated from ground by a custom designed voltage-to-current source. The current was measured across a 1 kΩ resistor in series with the animal.

2.5 Signal Recording, Storage, and Processing

The potentials resulting from the current injection were recorded by the signal averaging system. Potentials were amplified with a gain of 100 by an Ithaco model 1201 differential amplifier referenced to a far field electrode inserted subcutaneously at the hip. The potentials were sampled at a rate of 10 samples per cycle, 100 samples per stimulus. The onset of the stimulus and the sampling were triggered together so that sampling continued for the period of one cycle after the stimulus ended. Two hundred stimuli were presented and the responses were averaged. This average was stored so it would be available later for measurements of amplitude and phase with respect to the stimulus. Table 2 summarizes the stimulus and recording specifications for all three stimulus frequencies.

Table 2: Stimulus and Recording Specifications

f	Stimulus Time	Stimulus Rate	Sample Rate	Sample Time
100 Hz	90 ms	5 Hz	1 ms	100 ms
1 kHz	9 ms	50 Hz	100 μs	10 ms
10 kHz	0.9 ms	50 Hz	10 μs	1 ms

2.6 Stimulus and Recording Configurations

No useful data were obtained from the first four animals that were used to determine the effectiveness of the implantation procedure and to refine the experimental methods. The next series of animals was chronically implanted, meaning the animals were allowed to recover from surgery and studied over several weeks or months before being sacrificed. Chronically implanted animals were always anesthetized during experimental sessions with the same drugs used for the implantation procedure. They allowed for investigation of the effects of time and tissue growth inside the cochlea. Later implantations were acute, meaning that the implantation, data collection, and animal sacrifice were completed in one session, thus preventing any tissue growth and leaving the cochlea in a nearly normal state.

The first experiments designed to test the model used monopolar stimulation, stimulation between an intracochlear electrode and the ipsilateral pinna (the pinna on the side of implantation). Potential recordings were both monopolar, i.e., between each of the four remaining intracochlear electrodes and the contralateral pinna (the pinna opposite the side of implantation), and bipolar, i.e., between pairs of intracochlear electrodes. The stimulus potential, the potential between the two stimulating electrodes, was also recorded.

Bipolar recordings with monopolar stimuli were made to test the integrity of the electrodes and the correct operation of the stimulating and recording equipment. Combinations of the bipolarly recorded potentials with the monopolarly recorded potentials created many three-leg loops with potential measurements for all three legs. For example, monopolar recordings at the apical electrode and the mid-apical electrode produce a closed loop when combined with the bipolar recording between these two electrodes. Such potentials were summed to determine if the result would indeed

be 0 V, thus confirming that the "circuit" obeyed one of the basic laws of circuit theory.

The stimulus current intensity of 10 μA was initially chosen because it is a low intensity current that was in the same range as the 20 μA current used in the tests of the human model. Several animals, however, were presented with stimuli of varying intensities to check the linearity of the system. These intensity series used monopolar stimulation at the apical electrode and monopolar potential measurements at the mid-apical electrode. The stimulus intensities began at 1 μA, increased to 5 μA, and further increased in steps of 5μA up to 40 μA.

Normal recording runs at all three frequencies were done for three animals after death to determine the effects of death upon the recorded potentials. Two rats were sacrificed by injection into the brain stem of 0.05 ml sodium pentobarbital, which causes immediate cessation of respiration. Another rat died during the surgical procedure; however, the implantation was completed, so that the potential distributions could be measured several hours after death. With the two animals that were sacrificed by sodium pentobarbital injection, stimuli were applied at the apical electrode and monopolar potential recordings were made at the other electrodes every three minutes until 20 minutes after death. One of these animals was stimulated further at ten-minute intervals until 125 minutes after death.

Several animals were used to investigate the effect of the position of the return electrode upon the stimulating voltages and potential distributions. These experiments were done to determine if the difference between the position of the model stimulus return, at the brain stem, and the experimental stimulus return, at the ipsilateral pinna, would affect the comparisons between model generated data and the physiologic data. Opening the cranial cavity to expose the auditory nerve and brainstem also allowed us to ask whether such exposures might influence the patterns of current flow. This was of interest because studies in the cat of single auditory nerve fiber responses to electrical stimuli at the MEEI and other laboratories require such exposures. To make these investigations, terminal experiments were conducted on several animals. At the conclusion of all other planned experiments, the dura - the tough, protective tissue that surrounds the central nervous system - was exposed over the foramen magnum by removal of the soft tissue covering it. Another sequence of

monopolar stimulation and monopolar potential measurements was run. The base of the occipital bone was removed to expose the cerebellum, the dura over it was removed, and the cerebellum was aspirated away with light suction. After each successive tissue removal, a stimulus sequence identical to the first was run to investigate the possibility of any changes in the recorded potentials. When the cerebellum was removed, the auditory nerve was exposed from inside the skull and the return stimulating electrode was placed on it to produce a stimulus configuration that closely approximated that of the model.

Several animals were presented with bipolar stimulation, and measurements were made of the stimulating voltage. These experiments were conducted to test the hypothesis that the electrode-fluid interface of the cochlea was introducing a capacitive effect that was responsible for the different voltages required to drive the 10 μA current at different frequencies without affecting the recorded potentials at other electrodes.

2.7 Model Data Generation

Model data were generated by Dr. Meng-Yu Zhu. Preliminary estimates for positions of the electrodes were made on the basis of drawings of the positions of the holes in the capsule made during implantation and verified in the fixed material during the dissection of the cochleas for histological processing. Because electrode positions were uncertain, monopolar stimulation was implemented not only for scala tympani, but also for adjacent points in scala media and scala vestibuli. Potential as a function of position was plotted for each scala, thus producing nine data sets per electrode. The stimulus input to the model cochlea was 10 μA, as it was in the physiological experiments.

2.8 Animal Sacrifice and Histology

Most of the animals were sacrificed by intracardial perfusion with a formaldehyde-glutaraldehyde solution. The skull was removed and stripped of all external soft tissue. Bone tissue was removed to expose the posterior surface of the cerebellum and ventral surface of the brain stem. The skull was stored in the perfusion solution until the cochlea was harvested.

The animals involved in the experiments to investigate the effect of animal death were not perfused as all other animals were. Because each had been dead for several hours at the completion of the experiment, the skull was removed immediately, stripped of external soft tissue, and placed in the formaldehyde-glutaraldehyde solution.

The histological processing of the cochleas from the initial series of animals has been completed by Dr. Wen Z. Xu. The processing for the last series is not yet complete. In the processing, the cochleas were decalcified after dissection from the skull, perfused with osmium tetroxide (OsO_4), and embedded in araldite. They were then cut in 5-μm sections, placed on microscope slides, and stained with toluidine. Locations of the electrodes were determined in the first series of animals, RM5 to RM11, by locating the holes through which they were inserted and the tissues that surrounded them as a reaction to a foreign body. Electrode positions that are presented for the last series of animals are based upon estimations of the locations of the electrode holes using a low-power microscope to view the dissected cochlea. External cues such as the stria vascularis, which appears as a dark band beneath the capsule, were used to determine over which scala a particular hole was drilled. The scala over which an electrode hole appeared was assumed to be the scala in which the electrode tip had resided because an attempt was made to insert the electrodes so that they were perpendicular to the wall of the capsule. This attempt, if successful, would mean that the electrodes would not cross a scalar boundary once inside the capsule.

3 Results

Our original plan was to determine electrode locations in all of the animals in histological sections. This is possible in animals implanted for periods as short as one week because the electrode tip is surrounded by tissue that is part of a foreign body reaction. However, in the first series of animals, RM5 to RM11, it was clear that the new tissue growth in chronically implanted animals was considerable and might have been responsible for some seemingly anomalous results.

Consequently, the more recent subjects, RM19 to RM22, were not chronically implanted, but were acute preparations from which data were collected immediately after implantation.

Table 3 summarizes the electrode positions for each subject. Final verification of these electrode locations in subjects RM19 to RM22, will come when the histological processing is complete. Because these were acute preparations, there will not be tissue reactions to help us in locating the electrode tips. It will only be possible in most cases to verify the location of the electrode holes.

Table 3: Summary of Electrode Positions

Subject Number	Apical	Mid-Apical	Mid-Basal	Basal	RW
RM5	SV	SM	SM	ST	ST
RM7	SV	SM	SM	ST	ST
RM10	SV	SM	SM	ST	ST
RM11	SV	SM	SM	ST	ST
RM18	SV	SV	SM,SV	ST	ST
RM19	SV	SM	SM,ST	ST	ST
RM20	SV	SM	SV?	ST	ST
RM21	SV	SM	SM	ST	ST
RM22	SV	SM	SM	ST	ST

The basal electrode was inserted through the round window, and its insertion involved no drilling of the capsule. However, it left no external evidence of its position. Our hope was that the electrode would travel along the length of scala tympani to its resting position without damaging the scalar wall. However, the histological sections for RM5, RM7 and RM10, in which blunt tip electrodes were used for the basal electrode, revealed evidence that the electrode tip had ruptured the basilar membrane and crossed partly into scala media. A ball tip electrode was used for the basal electrode

in all later subjects in an attempt to minimize this sort of damage. The histological sections of the cochlea of RM11 revealed that this effort was only partly successful. There was very little damage in the region of the basal electrode, but the basilar membrane was ruptured over an extent of almost 0.5 mm.

As the table illustrates, insertion of the mid-apical and mid-basal electrodes into scala tympani was achieved very rarely. The area of scala tympani directly beneath the cochlear capsule was not substantially larger than the width of the electrode; thus, accurate positioning of the drill was very difficult. These electrodes were also positioned about 10° to 15° medially to the crest of the capsule. This medial position may explain the failure to implant successfully scala tympani, since the dorsal profile of scala tympani narrows considerably away from the midline in both directions.

The apical electrode was always placed in scala vestibuli. The original goal to insert it into the helicotrema, where scala tympani and scala vestibuli meet, would have placed the electrode in contact with both scalae. However, in addition to the problems of accurately positioning the drill, the apex of the cochlea was very difficult to drill because of its sharply convex surface. The drill tip would frequently slide away from the apex and enter the ventrolateral quadrant of scala vestibuli.

In much of the presentation that follows, the intended position of the electrodes has been used to designate electrode location. Potentials are plotted as functions of distance from the round window measured along the length of scala tympani. When the electrode under examination was not in scala tympani, the point in scala tympani that is radially equivalent to the electrode location is used as the reference for distance measurements. This adjustment is necessary because the scalae have very different lengths.

The discrepancies between intended electrode locations, which were all in scala tympani, and the actual electrode locations influences the data in a variety of ways. Locating an electrode in the wrong scala complicates comparisons with the model because it is not possible to make meaningful comparisons based upon model implementations with stimulation and recording in the same scala. One has to calculate the potential distributions for all scalae in which the electrodes reside. In practice, however, this was not necessary, at least for cases in which only electrodes three or four

positions away from the stimulating electrode were in different scalae. In these cases, the potentials in the three scalae seem to converge to the same potential regardless of which scala is stimulated. (See discussion on page 46.)

3.1 Bipolar and Monopolar Potentials with Monopolar Stimulation

Before model data were generated and compared with experimental measurements, several underlying assumptions of the model were tested. The model assumes that the system is linear over the range of stimulus intensities that might be used for stimulation; that capacitive effects are small and of no practical significance; and that the electrical "circuitry" of the rat's cochlea conforms to the basic laws of electrical circuits. The first assumption was tested in the intensity series experiments conducted in both the first (chronic) series and last (acute) series of animals. The second assumption was tested in the acute series of animals by stimulating the cochlea at various frequencies. The last assumption was tested in the first series of animals through bipolar and monopolar recordings made during monopolar stimulation to create circuit loops with potential measurements at all legs.

RM5, RM7, and RM10 were stimulated monopolarly at each electrode while potential measurements were made monopolarly at each of the other electrodes and bipolarly at each pair of intracochlear electrodes that did not lie on opposite sides of the stimulating electrode. This collection of monopolar and bipolar potentials was used to create many loops throughout the cochlea. The potentials around these loops were summed to determined if they summed to zero potential, as basic circuit theory would dictate.

Bipolar potentials recorded from RM5 eleven days after implantation are summarized in Table 4. Electrode positions have been abbreviated as follows: A = apical, MA = mid-apical, MB = mid-basal, B = basal, RW = round window, CLP = contralateral pinna, and ILP = ipsilateral pinna. These data are quite representative of the data collected from all three animals. All potentials summed around loops resulted in near zero potentials.

Table 4: Summary of Loop Potentials in RM5

Stim.	Rec.	V (mV)	Rec.	V (mV)	Rec.	V (mV)	V_{SUM} (mV)
A-ILP	MA-CLP	24.61	CLP-MB	-12.21	MB-MA	-12.61	-0.21
MA-ILP	MB-CLP	22.00	CLP-B	-3.98	B-MB	-18.28	-0.26
B-ILP	MB-CLP	4.08	CLP-MA	-3.63	MA-MB	-0.50	-0.05
RW-ILP	A-CLP	4.34	CLP-MA	-6.43	MA-A	2.11	0.02

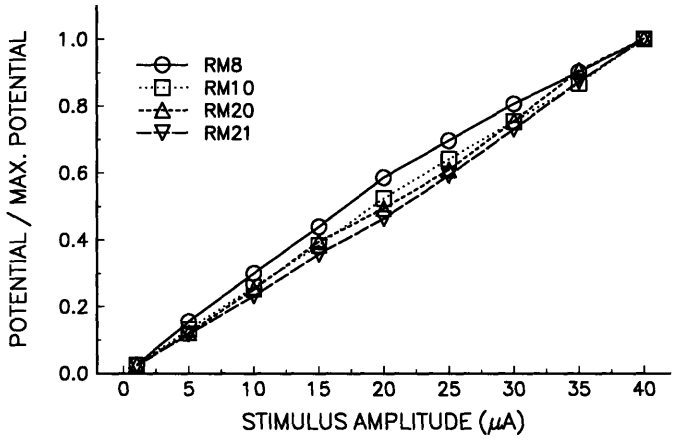

Figure 4: Intensity Series Data from RM8, RM10, RM20, RM21.

3.2 Intensity Series

The intensity series were run by stimulating monopolarly at the apical electrode beginning with 1 μA, increasing to 5 μA, and then increasing in 5-μA increments up to 40 μA. The potentials were recorded monopolarly at the mid-apical electrode. Figure 4 is a plot of these data.

The data were normalized by dividing all amplitudes from a particular animal by the potential recorded from that animal with 40-μA stimulation. This normalization made comparisons between animals possible despite large differences in the magnitude of potentials between animals.

The cochlea-electrode system exhibits a linear voltage vs current relation for stimulus currents up to approximately 20 μA. Above 20 μA, the relation remains linear, but its slope, i.e., the resistance, is different from that below 20 μA. The resistance changes varied from 0.06 kΩ in RM10 to 1.51 kΩ in RM21, but these changes accounted for only a small percentage of the total resistance in all

animals. One possible explanation of the resistance change is a breakdown of the electrode with high-intensity currents.

3.3 Stability of the Potential Distributions over Time

Several animals were implanted chronically and monopolar potential recordings were made during monopolar stimulation. In two of these animals, RM5 and RM10, the data were collected beginning at least one week after implantation. From RM11 data were collected immediately after implantation and again 3 days later. Figures 5, 6, and 7 are plots of these data. The data collected from RM5 and RM10 were collected over several months. The histological sections revealed that the scalae in both animals contained a great deal of fibrous tissue. The data from RM11 were collected within three days of implantation. In this animal there was virtually no abnormal tissue after this short interval.

The data of RM5 show a few inconsistencies over time, for example, the initially increasing then decreasing potentials at the mid-apical and mid-basal electrodes with apical stimulation. The large potential gradient between the basal and round window electrodes was also unexpected because these electrodes are not far apart in the basal turn of the cochlea, separated only by perilymph in the normal cochlea. In RM10, the potential distributions are similar to those of RM5 and show small reductions at many sites with time, and rather large reductions at the two most apical electrodes when the stimulus was at one of them. However, in both animals the overall shape of the distributions remained fairly constant. The data of RM11 show a small increase in potential at every electrode under every stimulus condition between the first and second recording sessions. The shapes of the distributions at these two times were very similar.

These data show that some instability does exist in the potential measurements over time, in both the magnitude and shape of the distributions. The extent of this effect that is due to tissue growth in the cochlea has yet to be determined in RM5 and RM10, but new tissue would not explain the changes in RM11 because little or no new tissue was present in that animal.

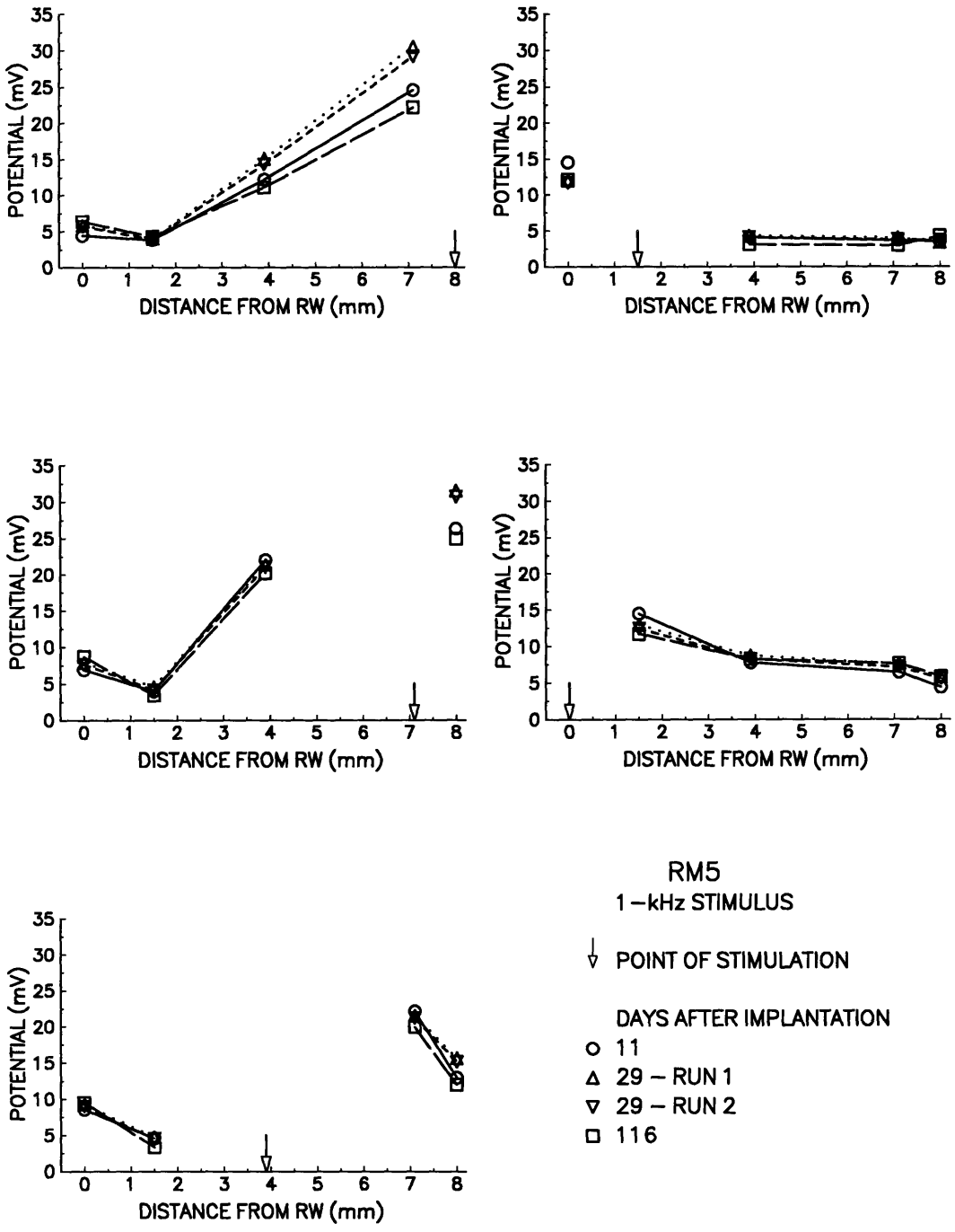

Figure 5: Monopolar potential distributions in RM5. The arrow denotes stimulation position along the length of the cochlea expressed as distance from RW along ST. Electrode positions in this and all succeeding figures are shown as the intended locations at the following distances: apical = 8.0 mm, mid-apical = 7.1 mm, mid-basal = 3.9 mm, basal = 1.5 mm, RW = 0 mm.

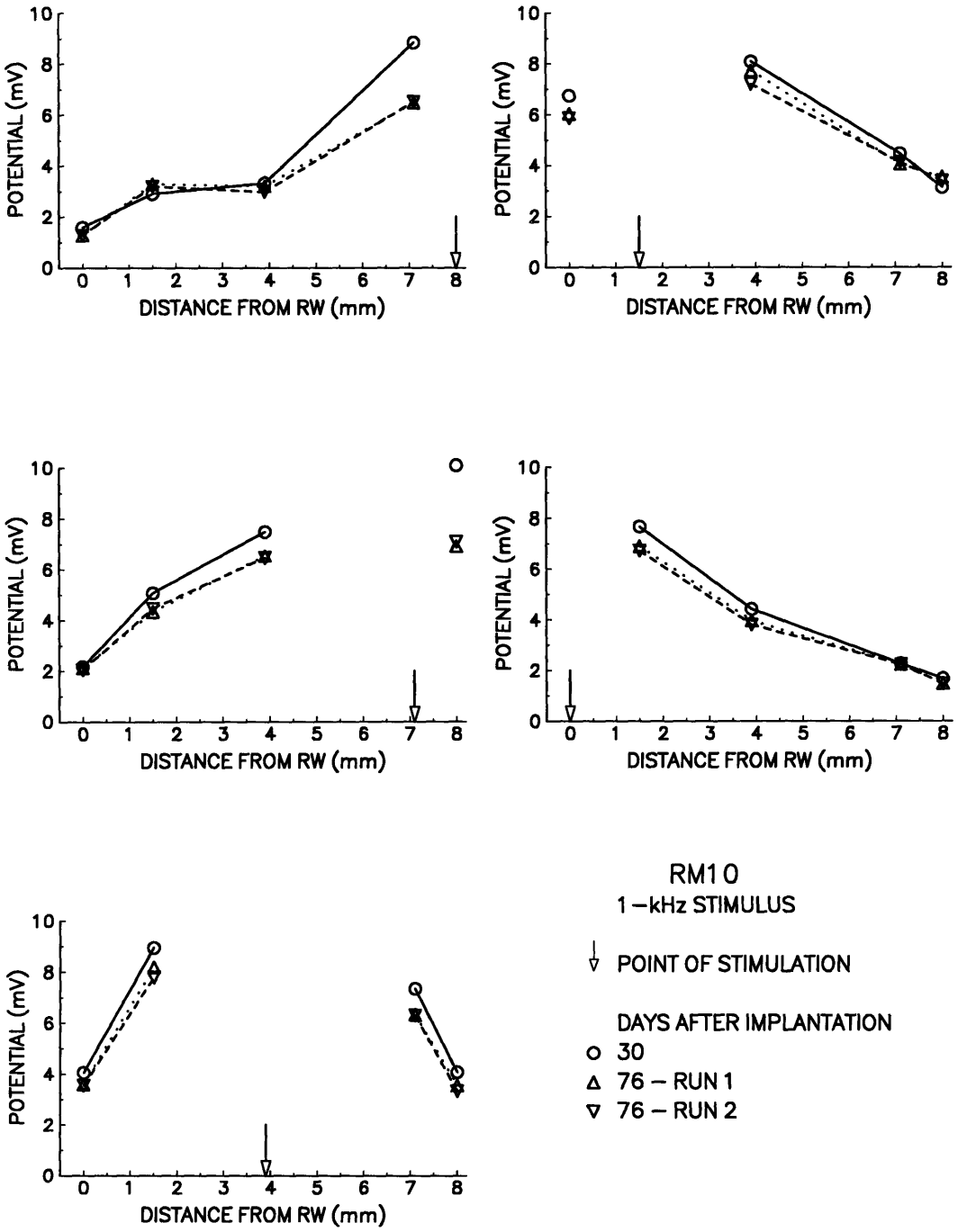

Figure 6: Monopolar potential distributions in RM10. Electrode positions are represented as in Figure 5.

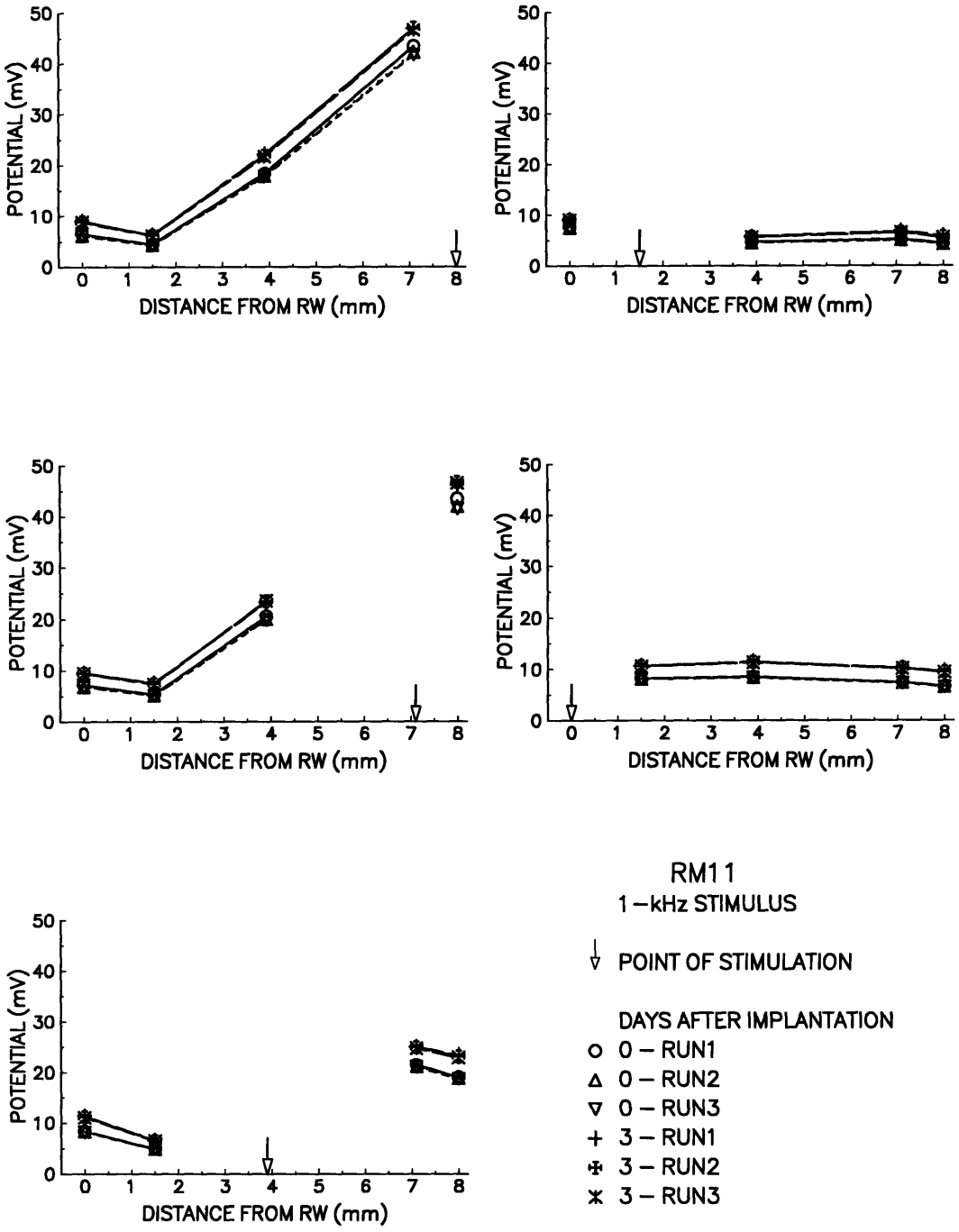

Figure 7: Monopolar potential distributions in RM11. Electrode postitions are represented as in Figure 5.

3.4 Effect of Death on Potential Distributions

Because of an interest in the possibility of an *in vitro* preparation for testing the model, the effect of death upon the potential distributions was investigated in two animals after sacrificing them with an injection of sodium pentobarbital into the brain stem. The cochleas were stimulated monopolarly at the apical electrode and monopolar potentials were recorded at each of the four remaining electrodes at various intervals. Figure 8 shows the changes following death in RM20 and RM22.

There were clear systematic increases in all of the potentials following the immediate cessation of breathing induced by the anesthetic injection. Although the changes in potential at the basal electrodes are not very clear in the plots of Figure 8, the percentage changes of the potentials at the basal end of the cochlea were substantial, with the basal electrode showing an increase of 16 percent in RM20 and 67 percent in RM21, and an increase of 18 percent in RM20 and 53 percent in RM21 at the round window electrode. Recordings from RM20 were stopped 21 minutes after death, while the potentials were steadily increasing. Recordings from RM22 were stopped after 125 minutes, after the onset of rigor mortus. The potentials recorded from RM22 seem to have stabilized.

Another rat, RM21, died during the implantation procedure, but the implantation was completed and data like those collected in the other animals of this recent series were recorded. They are shown in Figure 9, where it can be seen that the potentials were very large compared to those from all other animals. There was an apparent systematic dependence of the potential distributions on stimulus frequency, a result not found in any other animal, as will be shown later. Confidence in this result is low, however, because the stimulus isolator could not generate enough power to drive 10 μA through the cochlea at the 10-kHz frequency. Based upon the linearity data, a decision was made to stimulate with 5 μA and double the amplification of the resulting potentials, but it was not clear that this manipulation was without error. When the lower potentials at 10 kHz were discovered, the phase of the recorded waveforms relative to the stimulus waveform was measured. All recorded potential waveforms at this frequency were found to be in phase with the stimulus waveform. However, because the waveforms were sampled only ten times per cycle, the resolution

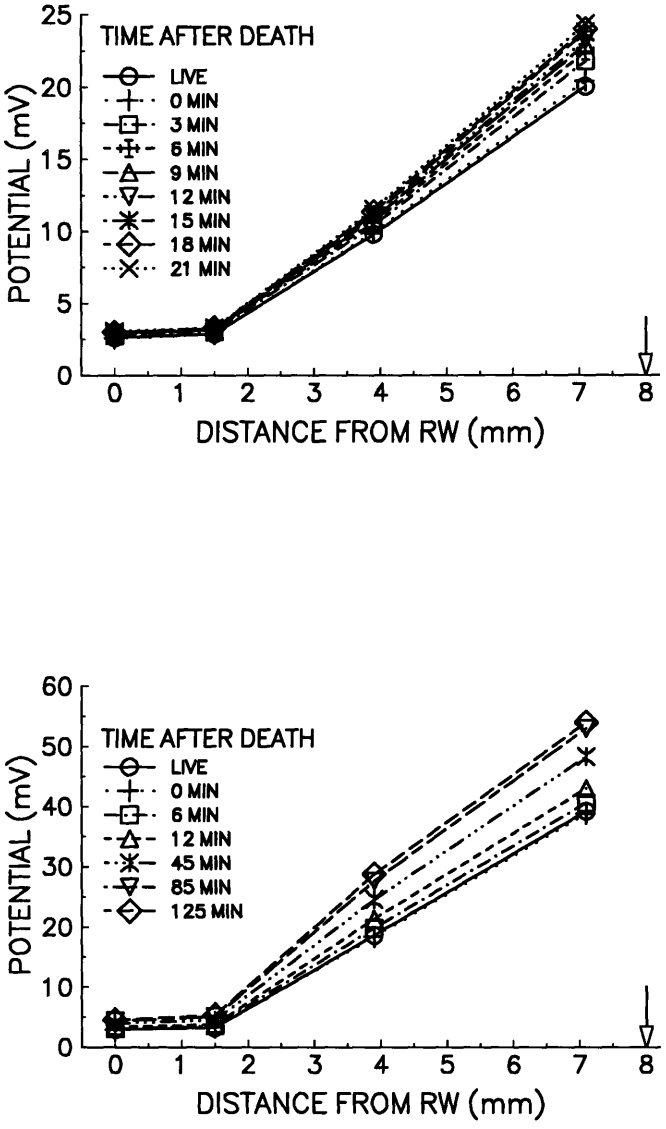

Figure 8: Monopolar potential distributions with apical stimulation from RM20, upper, and RM22, lower, at several times after death. Note the different scales of the y-ordinate in the two graphs. Electrode positions are represented as in Figure 5.

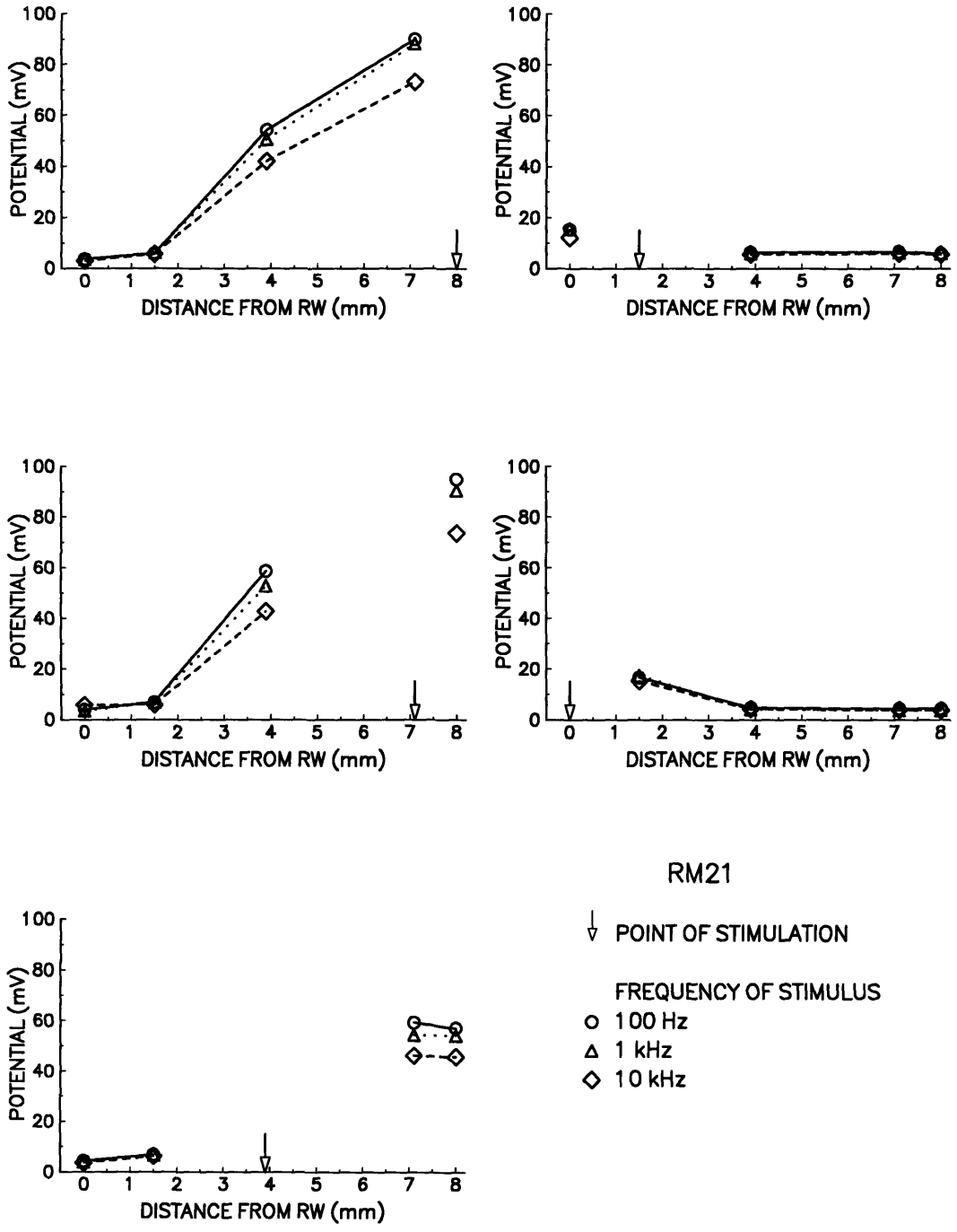

Figure 9: Monopolar potential distribtions in RM21, which had been dead for several hours before recording. Electrode positions are represented as in Figure 5.

of these phase measurements is only 36°.

3.5 Location of the Stimulus Return Electrode

The importance of the location of the stimulus return electrode was investigated to determine if the difference between this location in the physiological experiments and in the model implementations would affect comparisons of the two data sets. Because the internal auditory meatus was to be exposed in order to place a stimulating electrode there, it was possible to address another question of importance to the cochlear implant research done on cats; namely, whether opening the skull and removing some of the cerebellum, as is done in single auditory nerve fiber recording experiments, might alter the intracochlear potential distributions. These tests were run in terminal experiments on RM5 and RM10 by removing first the base of the occipital bone, then the dura, and lastly the cerebullum to expose the internal auditory meatus. After each stage of tissue removal, a monopolar stimulation run was made to investigate possible changes in recorded potentials that the tissue removal may have caused. When the cerebellum was partially excised, the return electrode was placed on or very close to the internal auditory meatus, and another series of recordings were made. In RM10, the return electrode was also driven through the brain tissue immediately after opening the skull to the approximate location of the auditory meatus. These data are plotted in Figure 10.

The potential distributions remained quite constant through the successive stages of tissue removal. The change in location of the return stimulating electrode (ground in the model) to the auditory meatus resulted in a very slight decrease in potential in RM5 at a few sights but a rather marked decrease in RM10, especially when the electrode was placed after exposing the internal meatus. With one notable exception, round window stimulation in RM5, the shape of the distributions remained rather constant in both cases.

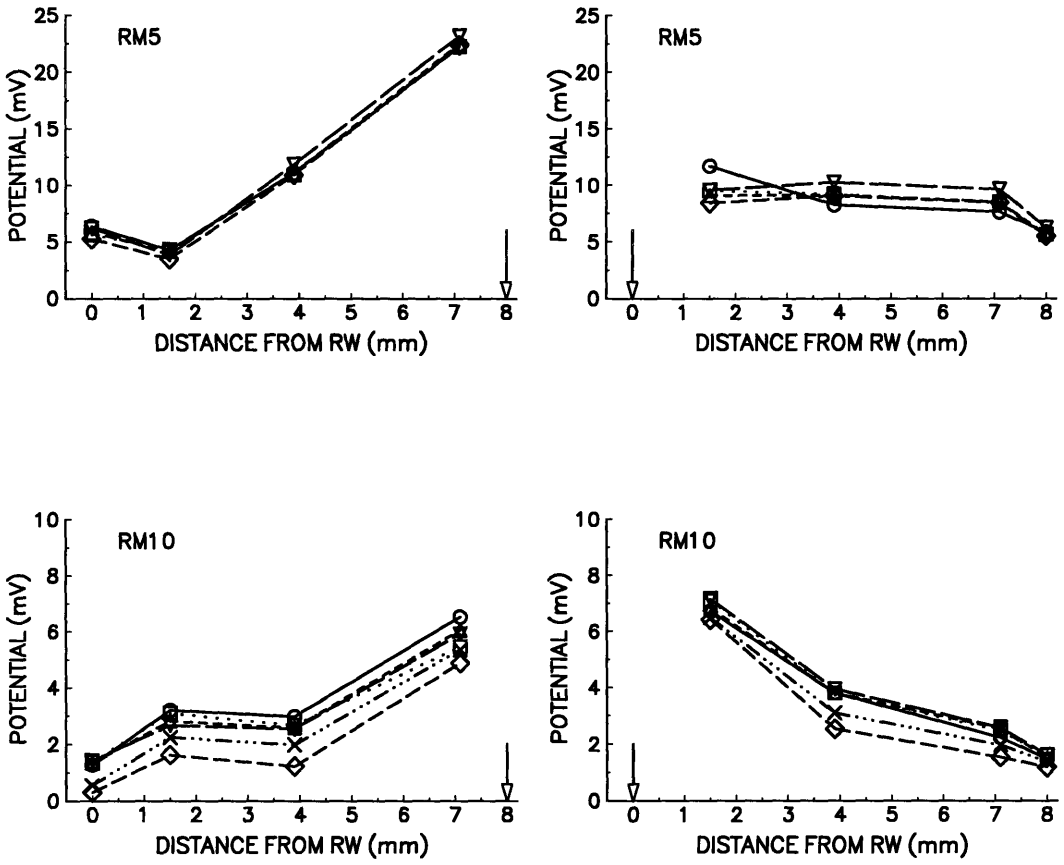

Figure 10: Monopolar potential distributions with apical and round window stimulation for RM5, upper panels, and RM10, lower panels. Only the posterior aspect of the occipital bone was removed. Electrode positions are represented as in Figure 5.

3.6 Effects of Stimulus Frequency on Potential Distributions

Three frequencies of stimulation, 100 Hz, 1 kHz, and 10 kHz, were used to investigate the possibility of capacitive effects within the cochlea in subjects RM18, RM19, and RM20. No 10-kHz data were collected from RM18. Two runs at each frequency were recorded from RM18 and RM20. RM19 was stimulated at each frequency for only one run. These data are plotted in Figures 11, 12, and 13. The phase with respect to the stimulus waveform was measured in several cases. The resolution of these measurements was only 36° because the potential was sampled only 10 times per cycle in order to reduce the computer memory needed to store the data. All potential waveforms were in phase with the stimulus waveforms, or at least less than 36° out of phase. These data, in conjunction with the general lack of frequency dependence in the potential distributions, seem to support the model assumption that there is no substantial capacitive effect with electrical stimulation in the rat cochlea.

The stimulus potentials for these animals, unlike the recorded potentials, were not invariant with stimulus frequency. Table 5 summarizes the stimulating voltages for the apical and round window electrodes in these animals. The variability in the required stimulating voltages across animals is probably due to differences in the implantation of each animal.

Table 5: Summary of Monopolar Stimulus Voltages Required for 10-μA Current at Different Frequencies

Subject	f (Hz)	Apical	RW
RM18	100	1020 mV	1050 mV
	1k	255 mV	295 mV
RM19	100	950 mV	550 mV
	1k	250 mV	140 mV
	10k	130 mV	80 mV
RM20	100	700 mV	720 mV
	1k	125 mV	120 mV
	10k	75 mV	65 mV
RM21	100	1100 mV	840 mV
	1k	410 mV	235 mV
	10k	120 mV	85 mV

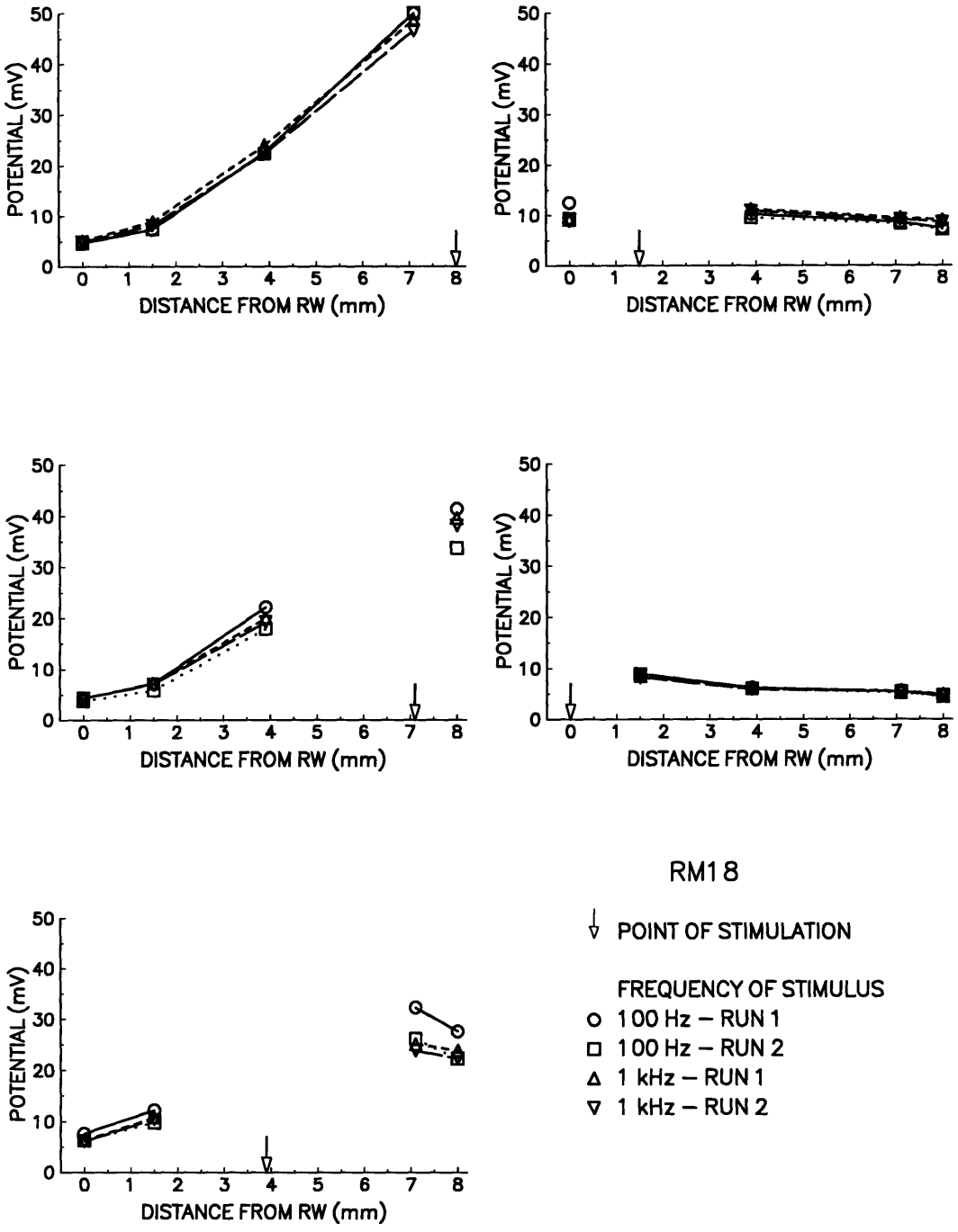

Figure 11: Monopolar potential distributions in RM18. Electrode positions are represented as in Figure 5.

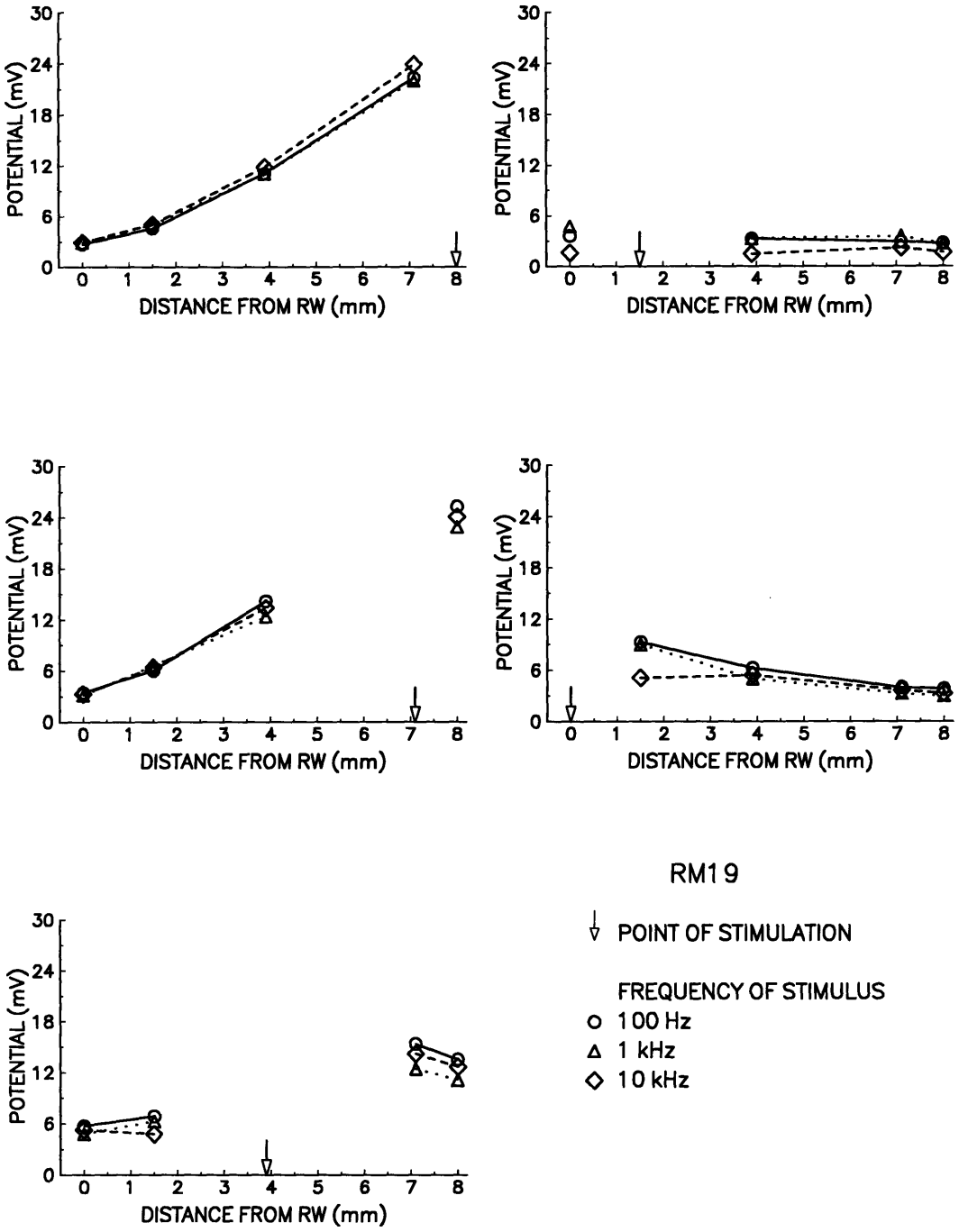

Figure 12: Monopolar potential distributions in RM19. Electrode positions are represented as in Figure 5.

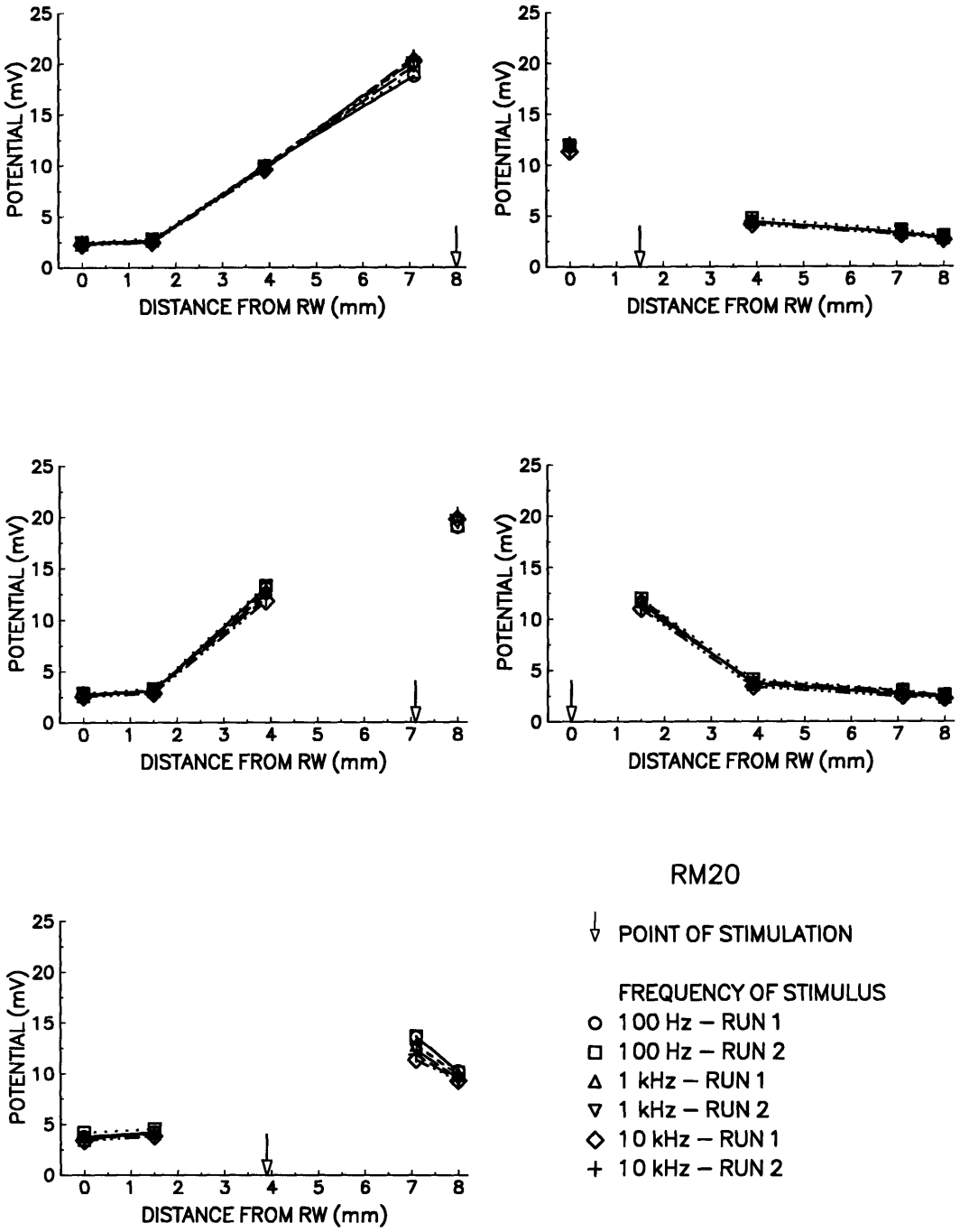

Figure 13: Monopolar potential distributions in RM20. Electrode positions are represented as in Figure 5.

The stimulating voltage between an intracochlear electrode and the ipsilateral pinna was dependent upon the frequency of stimulation. The potential decreased as the frequency increased, revealing some capacitance in the current path. Our initial ideas about the source of the capacitance attributed it to the tissues of the cochlea or the tissues that conduct the current from the cochlea to the ipsilateral pinna. The finding that the potentials measured in the cochlea did not vary systematically with frequency cast doubt on this idea. If that were the case, the recorded potentials would be affected by cochlear or other tissue capacitance because, as the stimulus potentials, they were measured across these tissues. If the capacitance were found in the tissues between the cochlea and the ipsilateral pinna, it should also affect the recorded potentials because the tissues between the cochlea and the two pinnae are very similar.

The similarity of the current paths between the cochlea and each pinna was investigated using RM22. The cochlea was monopolarly stimulated using the contralateral pinna instead of the ipsilateral pinna as the return electrode point. Table 6 compares the stimulating voltages when each pinna was used as the current return point.

Table 6: Stimulating Voltages at Each Electrode in RM22 Using Either Pinna as Current Return

Current Return	f (Hz)	Apical	Mid-Apical	Mid-Basal	Basal	RW
ILP	100	1040 mV	—	—	—	—
	1k	240 mV	165 mV	170 mV	460 mV	150 mV
	10	135 mV	—	—	—	—
CLP	100	1160 mV	790 mV	760 mV	1720 mV	720 mV
	1k	270 mV	175 mV	230 mV	475 mV	160 mV
	10k	145 mV	120 mV	120 mV	155 mV	85 mV

When the return electrode was in the contralateral pinna, the stimulus voltages were slightly larger than they were when the ipsilateral pinna was used. This increase is probably due to the longer distance between the stimulus and return electrodes when the contralateral pinna was the return point. The same frequency dependence was observed regardless of which pinna was used. These findings support the idea that the tissues between the cochlea and the two pinnae are electrically similar because they show that the capacitance in these pathways are similar; the same stimuli at

the several frequencies produce almost identical potentials.

The recording amplifier has a very large input impedance, so much less current flows through the pinna used as the recording reference than through the pinna used for stimulation. If the capacitance existed in the path from the cochlea to the pinna, and the current travelled only through the tissue connecting the cochlea to the stimulus return electrode, the capacitance would be observed only in the pathway of current flow, i.e. in the stimulus voltage but not the recorded potentials. However, the tissue of the head between the cochlea and the pinna was shown to be electrically uniform, so the current will distribute itself through all of the tissues rather than just a confined pathway.

The cochlea was stimulated bipolarly, i.e. between two intracochlear electrodes, to investigate frequency effects with this type of stimulation. Every pair of adjacent electrodes was bipolarly stimulated at 100 Hz, 1 kHz, and 10 kHz. The required stimulus voltages are summarized in Table 7 where it is clear that they showed the same dependence on frequency as the monopolar stimuli, decreasing markedly with increasing frequency.

Table 7: Stimulating Voltages with Bipolar Stimulation in RM22

f (Hz)	A-MA	MA-MB	MB-B	B-RW
100	1650 mV	1200 mV	2700 mV	2400 mV
1k	320 mV	310 mV	615 mV	540 mV
10k	95 mV	120 mV	210 mV	215 mV

Figure 14 is a circuit that was developed to explain the location of the capacitance and its effect only on the stimulus voltages based upon the measurements using bipolar stimuli. The bipolar stimulus potentials possess the same frequency dependence found under the monopolar stimulus conditions despite current paths that presumably consist mainly of highly conductive intracochlear fluid. The tissue resistances of the circuit model, RSTIS and RRTIS, are essentially the same, as mentioned before. The only point in the system not included in previous considerations was the path between the intracochlear stimulus electrode and the intracochlear recording electrode. This position of the capacitance would affect only the stimulus potentials and supports the conclusion that the capacitance must exist at the electrode-fluid interface of the intracochlear stimulating electrode, as

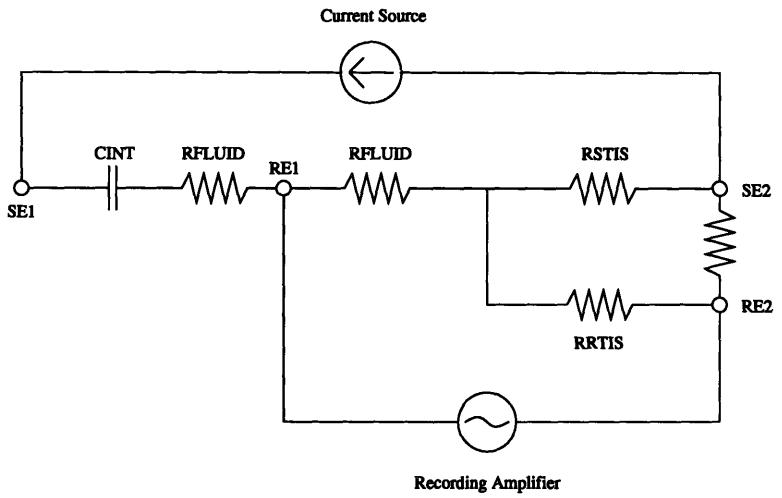

Figure 14: Circuit Model to Describe the Location of the Apparent Stimulus Capacitance: SE1,SE2 = Stimulus Electrodes; RE1,RE2 = Recording Electrodes; RFLUID = Intracochlear Fluid Resistance; RSTIS = Tissue along Stimulus Current Path; RRTIS = Tissue between Stimulus Electrodes

it is unlikely that it could exist in the resistive fluid of the scalae.

3.7 Monopolar Potential Recordings and Comparisons with the Model

One set of monopolar potentials was selected for comparison with the model from each animal in the last series, in which all of the potentials were recorded immediately after implantation to avoid complications introduced by extraneous tissue growth. Because all 1-kHz runs within an individual animal were very similar with respect to both distribution and magnitude, the first 1 kHz run from each subject was selected. The amplitudes of the potentials differed significantly across animals, as is evident from the previous figures. Figure 15 is a plot of the runs selected from each animal to further illustrate the differences in amplitude.

To permit comparisons across subjects with the model, the potentials were normalized by dividing all potentials from a particular animal by the largest potential recorded in that animal. With all subjects, the maximum potential was recorded at either the mid-apical electrode during apical stimulation, or at the apical electrode during mid-apical stimulation. The shape of the potential distributions was preserved by normalization, but the amplitudes were adjusted so that all distributions had identical peak amplitudes. Model comparisons were then made with the normalized data. Figure 16 summarizes the 1-kHz normalized potential data.

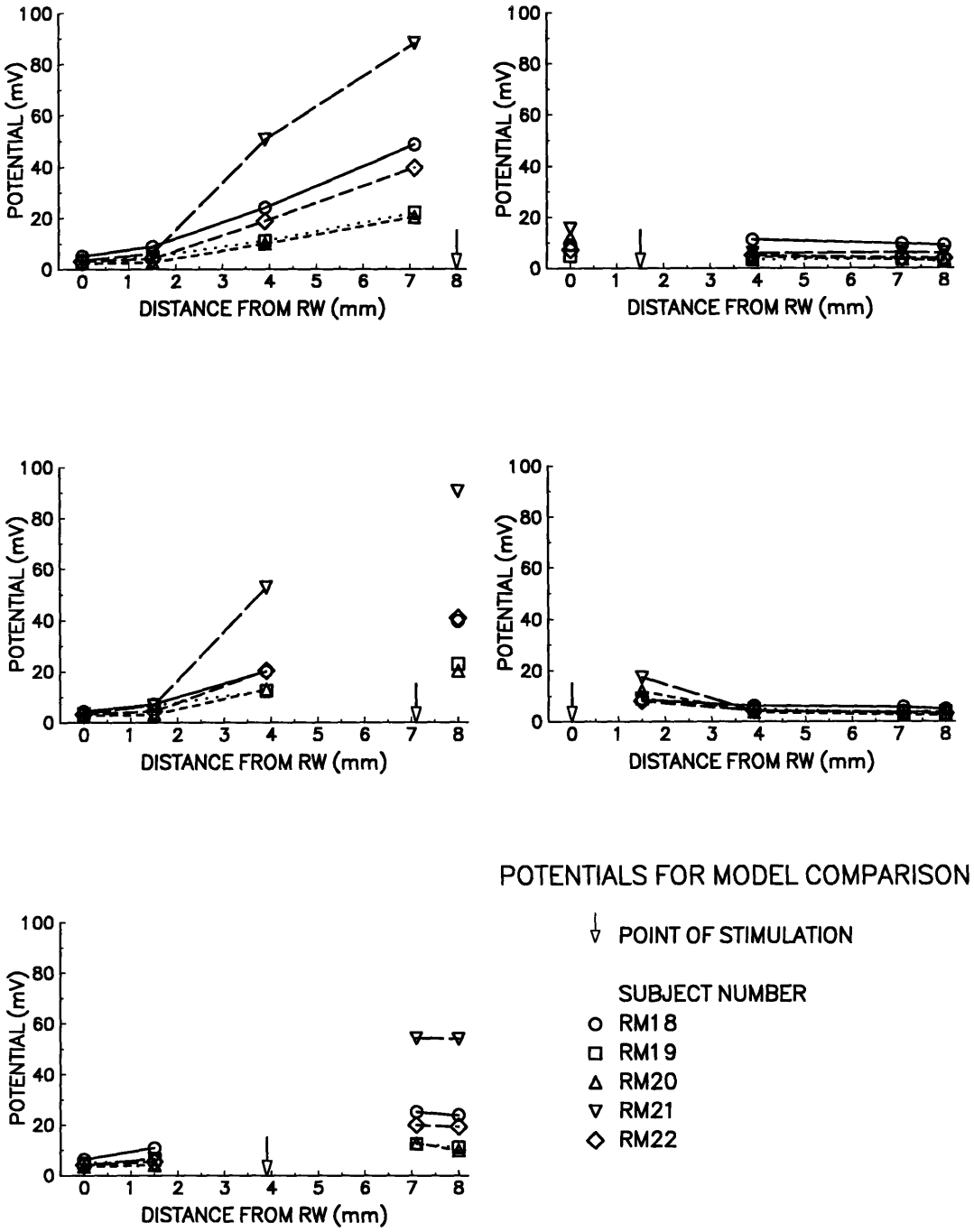

Figure 15: Monopolar potential distributions at 1 kHz chosen for comparison with model predictions. Electrode positions are represented as in Figure 5. RM21 was dead when the measurements were made.

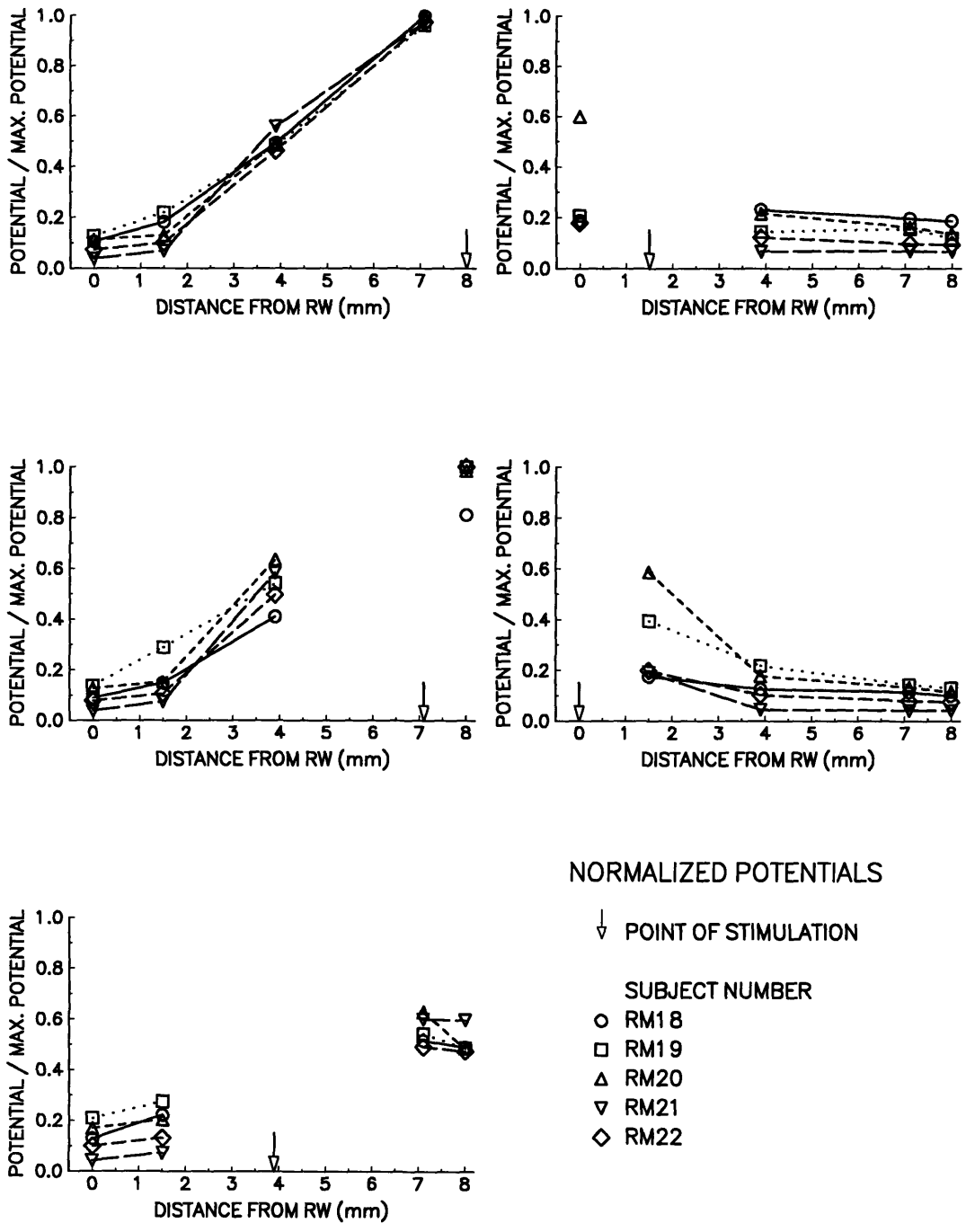

Figure 16: Normalized monopolar potential distributions in RM18, RM19, RM20, RM22. Electrode positions are represented as in Figure 5.

The model was run by Dr. Meng-Yu Zhu with stimulation applied at points that correspond to the electrode positions in the animals. It was necessary in these implementations to consider the possibility that the electrodes might not have been in the intended locations, as indeed the preliminary assessments indicated. Therefore, the positions of the electrodes around the cochlear spiral were transformed from distances along the length of scala tympani to degrees from the round window at 0° in scala tympani. This transformation allowed for model stimulation of the cochlea in different scalae at corresponding radial points. Changing the stimulating or recording points from one scala to another would have been difficult if distances from the round window were used because the scalae vary substantially in length. The resistivities of the model were chosen based upon previously published resistivity data. There are no published estimates of the resistivities of some kinds of tissues, so these resistivities were estimated using the values for similar types of tissue. Table 8 lists the different types of tissues and their resistivities used in the present implementations.

The model has two parameters to be estimated from the experimental data, a multiplicative one that controls the range of potentials, and an additive one that allows shifting the distribution to obtain the best fit. The additive factor simply represents a change in the location of the reference potential and is necessary because the model and experimental data do not share a common reference. The multiplicative factor adjusts the range of the model potentials to approximate that of the experimental measurements. For the present comparisons, the multiplicative factor was set using potentials recorded in scala media with stimulation in scala vestibuli at the apical electrode. These scalae were chosen because the apical electrode was in scala vestibuli in all animals, and it appeared that the mid-apical and mid-basal electrodes were in scala media. Though the basal and round window electrodes were not in scala media, the model data predicted that the potential distributions in each scala nearly converged at the basal end of the cochlea regardless of which scala was stimulated apically.

It should be noted that the mode of convergence in the model varies depending upon the direction of movement away from the stimulus location. Figure 17 illustrates this point. With apical stimulation (top panel of Figure 17) in each of the three scalae, the potentials along a particular

Table 8: Tissue and Fluid Resistivities of the Rat Model

Tissue of Fluid Description	**Resistivity in Ωcm**
Scala Vestibuli Perilymph	50
Scala Tympani Perilymph	50
Scala Media Endolymph	50
Ampullar Perilymph	50
Bone and Nervous Tissue of Modiolus	300
Spiral Ganglion Cells	300
Fluid Filled Space between Bone and Brain Stem	300
Modiolar Nervous Tissue	300
Brain Stem and VIIth Cranial Nerve	300
Cerebellum	300
Spiral Ligament	300
Bone and Nervous Tissue of the Osseous Spiral Lamina	300
Stria Vascularis	300
Organ of Corti	500
Tectorial Membrane, Limbus, and Dense Soft Tissue	5000
Basilar Membrane	5000
Bone Surrounding Scalae	5000
Otolith	5000
Loose Soft Tissue	5000
Round Window Membrane	5000
Scala Media Boundaries	20000
Oval Window, Reisner's Membrane, and Vestibule Membrane	20000
Air Filled Space	32000

scala rapidly converge at slightly more basal sites regardless of which scala is stimulated. The potentials in each of the three scalae also converge with stimulation in a particular scala, though the convergence is not as great. With movement in the apical direction with basal stimulation in a particular scala (lower panel of Figure 17), the potentials along the different scalae converge very rapidly. The potentials recorded in one scala with stimulation in each of them also converge, but to a much smaller degree. Though the convergence patterns do vary, all potential distributions in all scalae converge to within 0.1 normalization units at one end of the cochlea with stimulation in any scala at the other end.

The potentials recorded at the mid-apical and round window electrodes were used to set the multiplicative parameter. All model data were first shifted down by some additive constant so that the potential at the round window electrode became the zero potential point, thus reducing the scaling of the data to a simple multiplication or division. The model data were multiplied by the inverse of the difference between the average mid-apical and average round window potentials recorded from the experimental subjects. The multiplication resulted in model potentials whose mid-apical to round window potential difference equaled the average potential difference between these two electrodes in the experimental data. The additive factor by which all model data were shifted into best agreement with the experimental data was determined by finding a shift that would provide widespread agreement between model data and experimental data. The comparisons presented here were made by implementing model stimulation in the scala in which each electrode was presumably located, and recording in the first analysis along scala media. Figure 18 shows the intial comparisons that were made between the model and experimental data. The initial shift factor to bring the round window electrode to zero potential was -2.57 mV. The scale factor by which the model data were multiplied was 0.1938 $(\text{mv})^{-1}$. The shift factor required to bring the scaled model data and normalized experimental data into best agreement by a qualitative perceptual criterion was 0.15.

In a qualitative way the model predicts most of the distinctive features of the potential distributions: the steep gradients in the potential distribution that result with stimulation at the apical

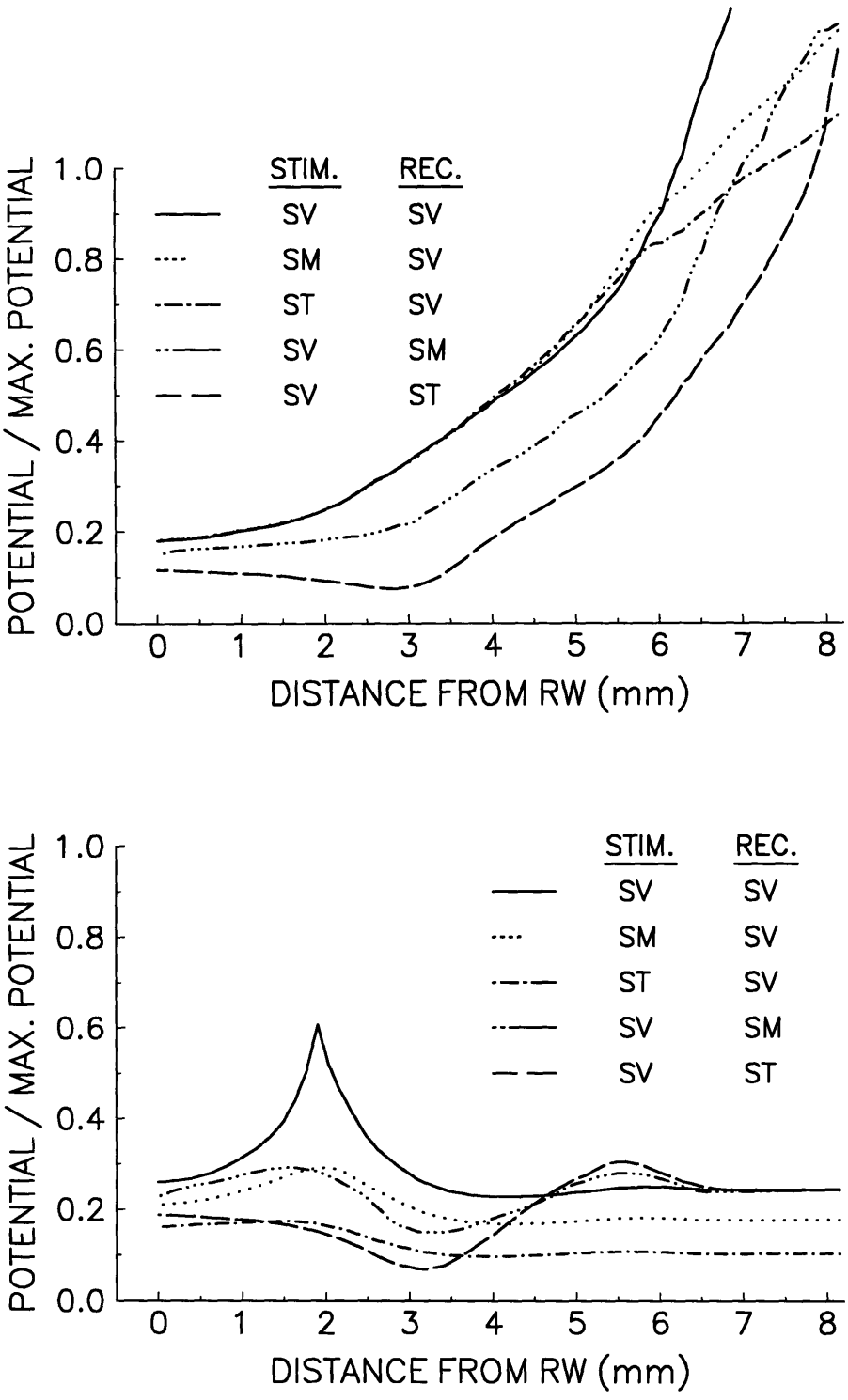

Figure 17: Model potential predictions for several stimulus and recording conditions.

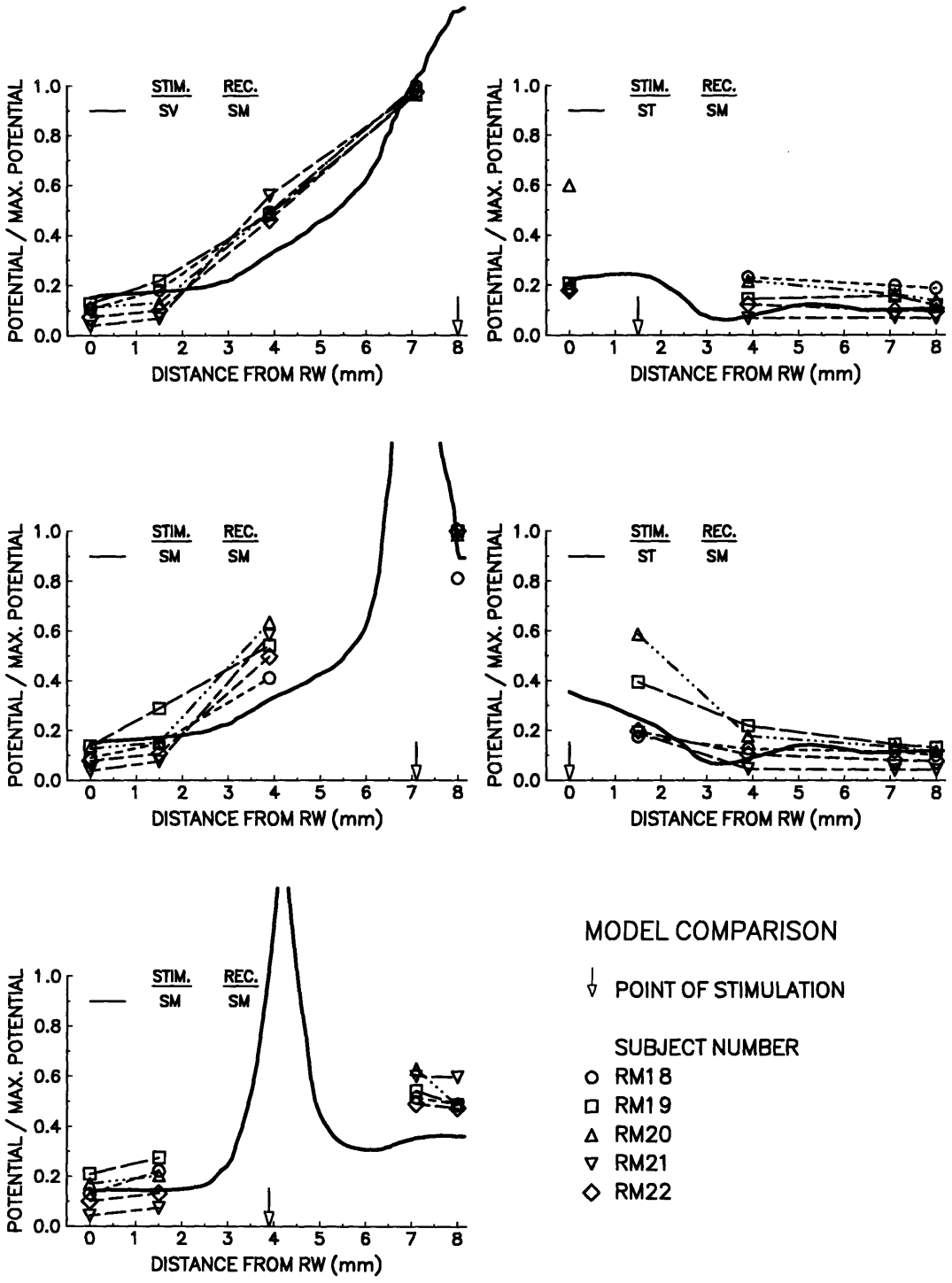

Figure 18: Initial comparisons between normalized experimental potentials and scaled model potentials along scala media. Electrode positions are represented as in Figure 5.

and mid-apical electrodes; the very shallow gradients that result from basal and round window stimulation, including the increased gradient between the mid-basal and basal electrodes with round window stimulation; and the higher apical and mid-apical potentials relative to the basal and round window potentials with mid-basal stimulation.

In this initial analysis, however, there are clearly discrepancies between the model and experimental data at several places. The predicted potential is significantly lower than the experimental potentials at the mid-basal electrode for both apical and mid-apical stimulation. While the model does predict the potential difference between the two most apical and two most basal electrodes with mid-basal stimulation, the magnitude of the difference is clearly underestimated.

Because the initial discrepancies between the experimental and model data seemed centered around the mid-basal electrode, the experimental potentials at this site were compared to model potentials for stimulation and recording in scala vestibuli. It became clear in the model implementations like those in Figure 18 that the scala vestibuli potentials should be significantly higher than scala media potentials under the conditions in which the discrepancies appeared. Figure 19 uses the same analysis except the model's predictions for scala vestibuli have been added in each panel and stimulation at the mid-basal location in scala vestibuli is included in the bottom left-hand panel. Although the mid-apical electrode was placed in scala media in nearly all animals, and the basal and round window electrodes were located in scala tympani, the practice of using model measurements from only one scala is acceptable because, as noted in the intitial comparisons, the potentials converge at points distant from the point of stimulation.

These new implementations assume that the mid-basal electrode is in scala vestibuli, not in scala media as we had supposed. That assumption seems to be borne out by the very improved agreement between model scala vestibuli potentials and the experimetal data at the mid-basal electrode with apical and mid-apical stimulation (top two left-hand panels of Figure 19). With scala vestibuli stimulation at the mid-basal site, the potential measurements at the two most apical locations are all brought into much closer agreement with predicted values (bottom left-hand panel of Figure 19). The histology of RM18 has just recently been completed, and the mid-apical electrode was found to

be in scala media, not scala vestibuli as this last analysis assumed. However, Reisner's membrane was ruptured in the immediate vicinity of the electrode tip over an extent of nearly 0.5 mm, opening the high resistance barrier between the two. It is not clear that this should make the electrode appear as one in scala vestibuli, but the model will be run to see if a break in the membrane would lead to such a result. If that turns out to be true, confidence in the model will be greatly increased.

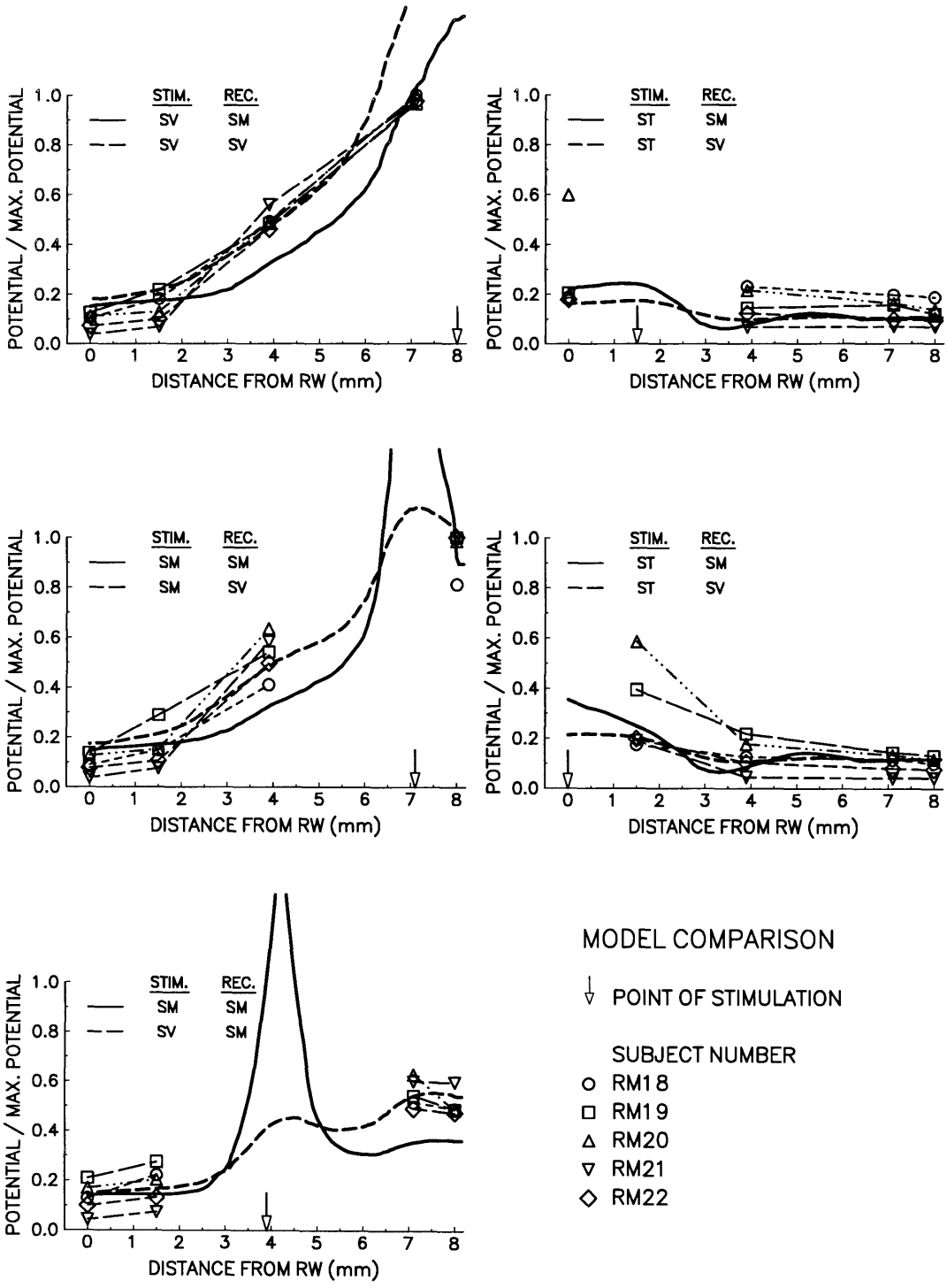

Figure 19: Normalized monopolar potentials compared to scaled model potentials along scala media and scala vestibuli. Electrode positions are represented as in Figure 5.

4 Discussion and Conclusions

The first experiments were designed to test some underlying assumptions of the model; namely, conformance of the implanted cochlea to basic circuit laws, system linearity, and independence of stimulus frequency. In general, these assumptions were all supported by the experimental data. The near zero potentials recorded around circuit loops within the cochlea were within the range of measurement errors. The system appeared linear up to a current level of 20 μA where a slight change of slope was seen. The basis of this apparent change in resistance is not clear, but it seems too small to be of much practical significance.

The data on the effects of stimulus frequency indicate that the capacitance of cochlear tissues does not greatly affect potential measurements of the kind made here. The decreasing stimulus voltages needed to drive currents of a given amplitude probably suggest a capacitance at the electrode-fluid interface in the stimulus circuit. It would be useful to determine the physical basis of this property, possibly as an aid for eliminating it with better electrode design.

Potential changes with time were observed in the chronically implanted animals, RM5 to RM11, but the changes were surprisingly small for the most part considering the large amount of tissue growth in two of the animals. Only slight variations in the potential distribution near the point of stimulation were observed. The short-term chronic implant (RM11) produced potential distributions that were slightly higher. The cause of this shift is unknown, but it cannot be attributed to new tissue growth as there was none in the histological sections for this animal. Clearly, the effects of new soft tissue and bone on the electrical properties of the cochlea is a matter of importance in cochlear implant research, as the cochleas of the deaf often are found in such conditions. The few data presented here suggest that the changes in potential distributions may not be very great, but it will be important to see if they can be reasonably simulated by the model.

The stimulus return location seemed to have little effect upon the potential distributions, validating the decision to use the ipsilateral pinna as the return electrode in these experiments even though the model predictions were referenced to the brain stem. There was a small decrease in potential when the stimulus return electrode was moved from the ipsilateral pinna to the internal auditory

meatus, but the change was very small and did not affect the shape of the potential distributions. The decrease was probably due to the shorter stimulus current pathway. The tissues of the head that the potentials were recorded across served as a current path when the ipsilateral pinna was the location of the stimulus return. When the return was moved to the internal auditory meatus, the potential across the tissues of the head was effectively zero because very little current flowed along that pathway.

The data also show that removing the brain tissue to expose the internal auditory meatus has little effect upon the electrical properties of the cochlea and auditory nerve. The slightly lower recorded potentials can probably be attributed to the pool of cerebrospinal fluid that collected in the cavity. The pool probably shunted part of the stimulus current pathway. However, these changes were slight and apparently occurred extracochlearly because no changes in the shape of the potential distributions were observed. This finding implies that extracochlear changes in the living organism, even severe ones, have little effect upon the intracochlear potential distributions.

The initial comparisons between the model predictions and the physiological data are very favorable. The model does a reasonably good job of predicting the potential distributions in the cochlea. The interesting discrepancies that seemed to be explained by the placement of one electrode in a different scala, thereby fitting the model predictions nicely, have not yet been explained. They may be if it can be shown that a ruptured Reisner's membrane effectively short circuits scala media and scala vestibuli, thereby making a scala media electrode behave as one in scala vestibuli. It will also be necessary to show for the other animals in the last series that something similar has happened in all of them. This will have to wait for the completion of the histological material. Future comparisons should investigate the model's capability to predict potentials in the damaged cochlea or one that has been substantially altered by tissue growth. Confidence in the model would grow if it is deemed effective when predicting the potential distributions of these abnormal states.

The experiments investigating the effect of death on the potential distributions support further investigation into the development of an *in vitro* preparation for further studies of the model. *In vitro* preparations, if deemed appropriate, would be very useful for generating experimental data

for model comparisons because they would afford much greater access to all points of the cochlea, especially the most ventral and medial aspects of the structure. Death seemed to have little effect upon the shape of the potential distributions, though the overall magnitude of the potentials was shown to grow after death. The investigations of return electrode location indicate that dissection of the cochlea from the skull may not affect the electrical properties of the structure. However, investigation of the effects of fluid loss, changes in ion concentrations, and long term effects of tissue death must be investigated before an *in vitro* preparation is likely to prove useful in studies of the cochlea's electrical properties.

References

Burda, H., Ballast, L., and Bruns, V. (1988) "Cochlea in Old World Mice and Rats (Muridae)," Journal of Morphology, **198**, 269-285

von Bèkèsy, G. (1951) "The Course Pattern of the Electrical Resistance in the Cochlea of the Guinea Pig (Electro-Anatomy of the Cochlea)," *Experiments in Hearing*, McGraw-Hill, New York, 1960

Girzon, G. (1987) *Investigation of Current Flow in the Inner Ear During Electrical Stimulation of Intracochlear Electrodes*, EE MS Thesis, MIT, Cambridge, MA